13. Other microstructural analysis methods

Contents

Contents

13.1 Ion probe microanalysis

- The ion probe uses electron optical methods to accelerate and focus primary ions into small high-energy ion beams to bombard the sample surface, excite and sputter secondary ions, and undergo acceleration and mass spectrometry analysis. The diameter and depth of the analysis area are 1~2 μm, Less than < 5 nm. It is an instrument for surface composition analysis.

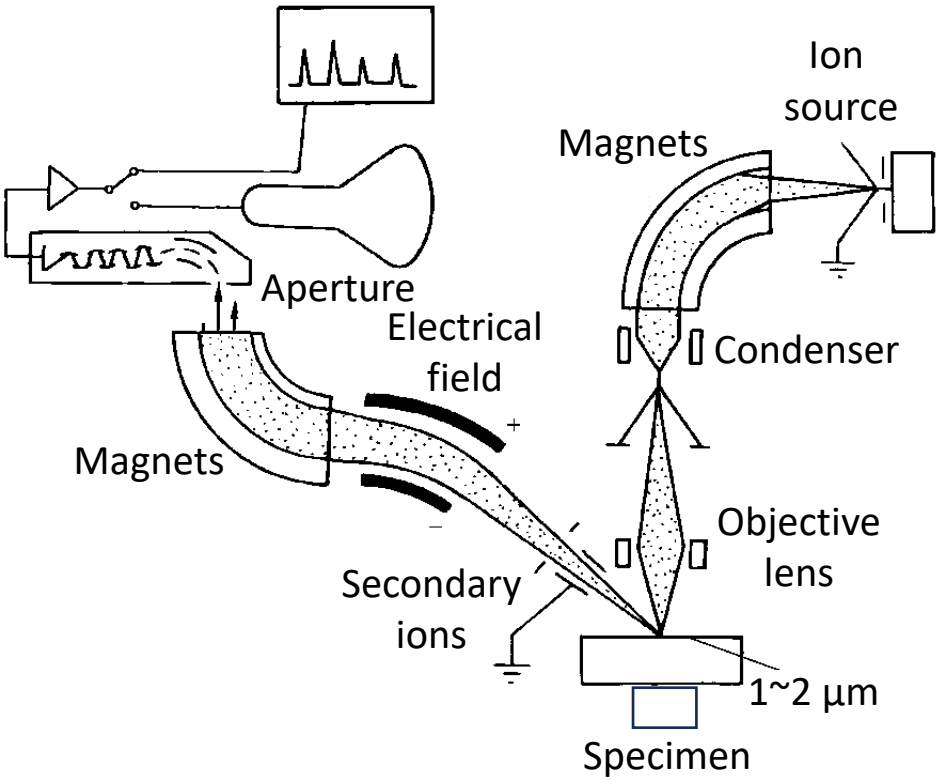

The structure of the ion probe is shown in the figure. The plasma flow generator ionizes the gas with an acceleration voltage of 12~20 kV. After being deflected by the sector magnet, it is focused into a small primary ion beam by the electromagnetic lens and bombards the selected sample analysis point.

13.1 Ion probe microanalysis

- First, the secondary ions enter the cylindrical capacitor electrostatic analyzer with a radial electric field ***E***, and the radius of the movement trajectory ***r'*** is:

$$r' = mv^2/Ee$$

In the formula, ***e*** and ***m*** are the ion charge and mass; ***v*** is the ion velocity.

- Subsequently, the secondary ions enter the uniform magnetic field in the sector magnet (magnetic induction intensity is ***B***) and are classified according to ***e/m***. If the accelerating voltage to induce secondary ions is ***U***, then the radius ***r*** of the ion trajectory in the magnetic field is:

$$r = \sqrt{\frac{2Um}{eB^2}} \propto \frac{1}{\sqrt{e/m}}$$

The ion trajectory radius ***r*** is inversely proportional to the square root of the secondary ion charge-to-mass ratio $(e/m)^{0.5}$.

- Finally, the signal is amplified to obtain the ion probe mass spectrum.

13.1 Ion probe microanalysis

The picture shows a typical ion probe mass spectrometry analysis result. The primary ion is 18.5 keV oxygen ion, and the sample is a silicon semiconductor.

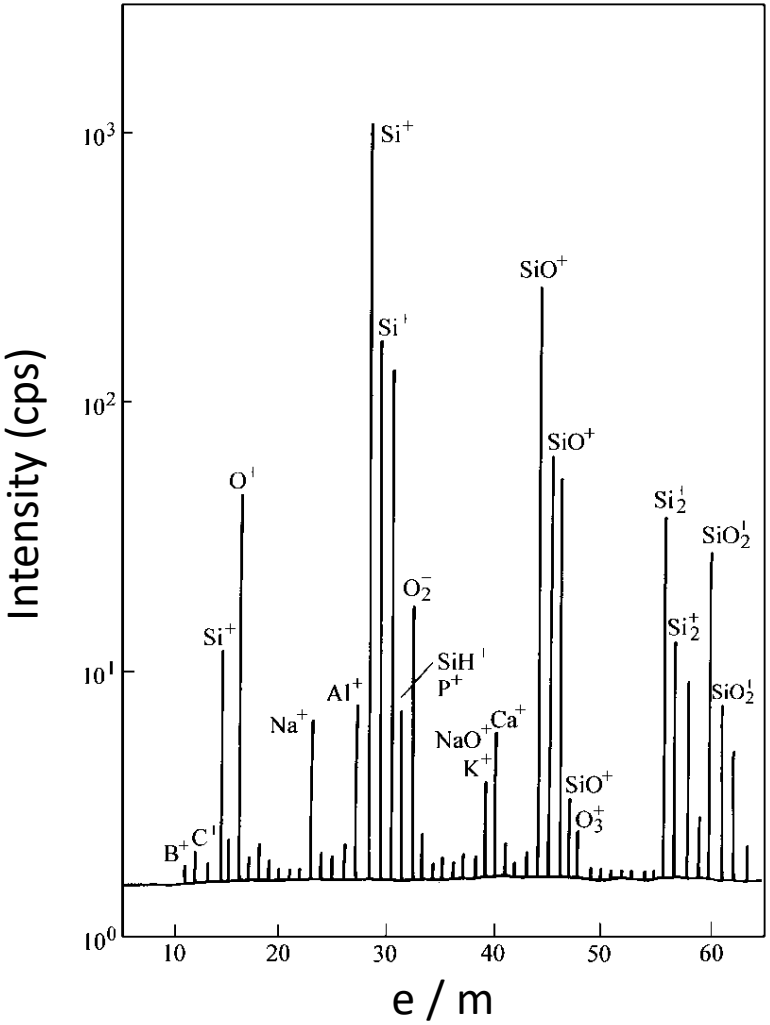

The background intensity of mass spectrometry analysis is almost zero, so its detection sensitivity is high, and the detection mass limit reaches the order of 10^{-19}, which is equivalent to hundreds of atoms using primary ion sputtering to strip layers, and the changes in element concentration with depth can be obtained.

When primary ions are scanned on the sample surface, a certain ion signal is selected for modulation imaging, and the surface distribution image of the element can be obtained.

13.2 Low energy electron diffraction analysis

- The incident electron energy of low-energy electron diffraction is 10 ~ 500 eV
- The sample that participates in diffraction only has one atomic layer on the surface. Even if the electron energy is high (≥ 100eV), it is limited to 2 to 3 atomic layers. It participates in diffraction in a two-dimensional manner, which is insufficient to constitute three-dimensional diffraction.
- The two-dimensional diffraction characteristics make it an important tool for solid surface structure analysis.
- For low-energy electron diffraction, it is important to keep the sample's surface clean to avoid additional diffraction effects due to impurity adsorption.
- During the diffraction analysis process, it is required that the surface contamination level is always lower than 10^{12} impurity atoms/cm^2. Therefore, an oil-free vacuum system must be used, and the vacuum degree should be better than 1.33×10^{-8} Pa.

13.2 Low energy electron diffraction analysis

As shown in the figure, when an electron wave with wavelength λ is vertically incident on a one-dimensional point sequence (the translation vector is ***a***), the scattered waves will strengthen each other in the backscattering direction that intersects an angle φ with the incident opposite direction, satisfying:

$$a\sin\varphi = h\lambda$$

In the formula, ***h*** is an integer. If the two-dimensional lattice translation vectors are ***a*** and ***b,*** respectively, then another diffraction bar needs to be satisfied.

$$b\sin\varphi' = k\lambda$$

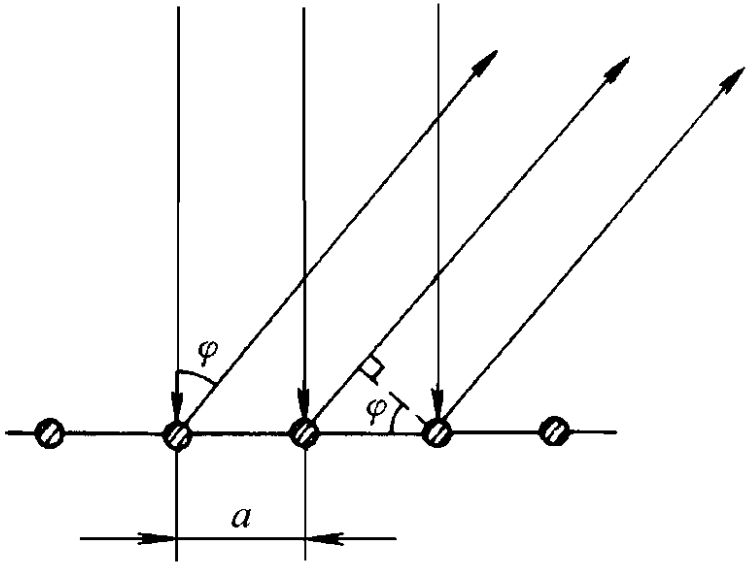

The above two equations are called two-dimensional Laue conditions. Under this condition, the diffraction direction is the intersection of two conical surfaces with the incident opposite direction as the axis and φ and φ' as the half apex angles.

13.2 Low energy electron diffraction analysis

- Diffraction of two-dimensional lattice

As shown in the figure, the radius of the Ewald sphere is $1/\lambda$, g_{hk} corresponds to the reciprocal rod of the reciprocal array point G and crosses the reflection sphere at A and A', and the diffracted wave vector in the backscattering direction is k', then we have:

$$k' \sin\varphi = g$$

$$d \sin\varphi = \lambda$$

Equation is Bragg's law of two-dimensional lattice diffraction.

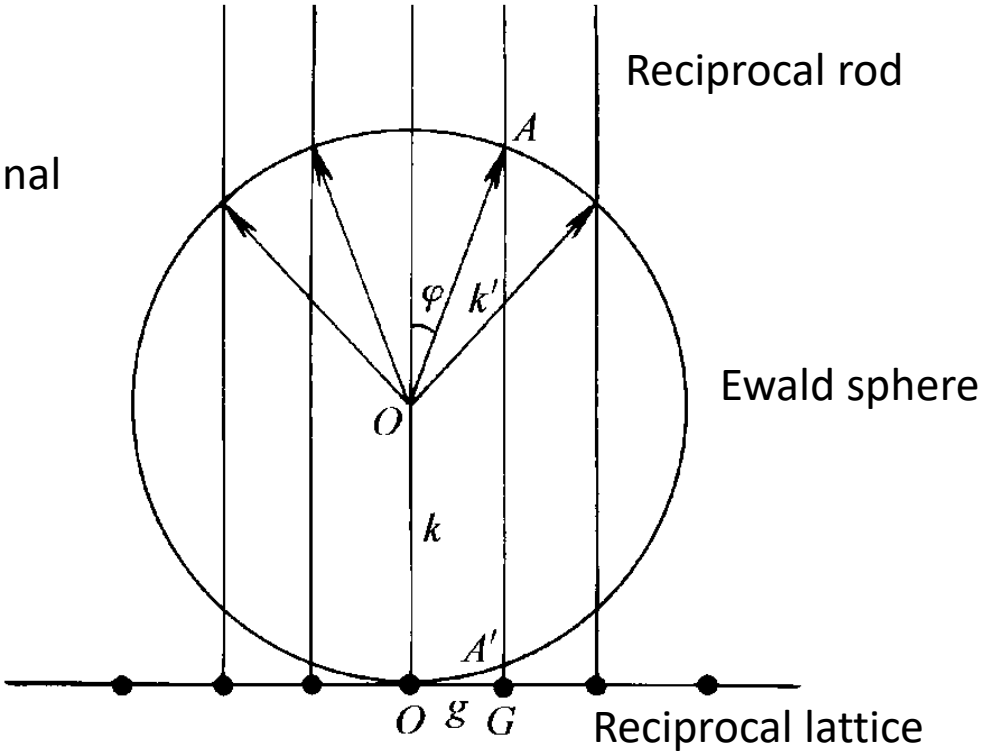

13.2 Low energy electron diffraction analysis

- Diffraction of two-dimensional lattice

As shown in the figure, if the surface atoms are arranged in an orderly manner, and the spacing in the direction of the matrix translation vector is ***2a*** and ***2b***, then the reciprocal translation vectors are ***a*/2*** and ***b*/2***, and a superstructure appears in the reciprocal lattice—array points (open circles).

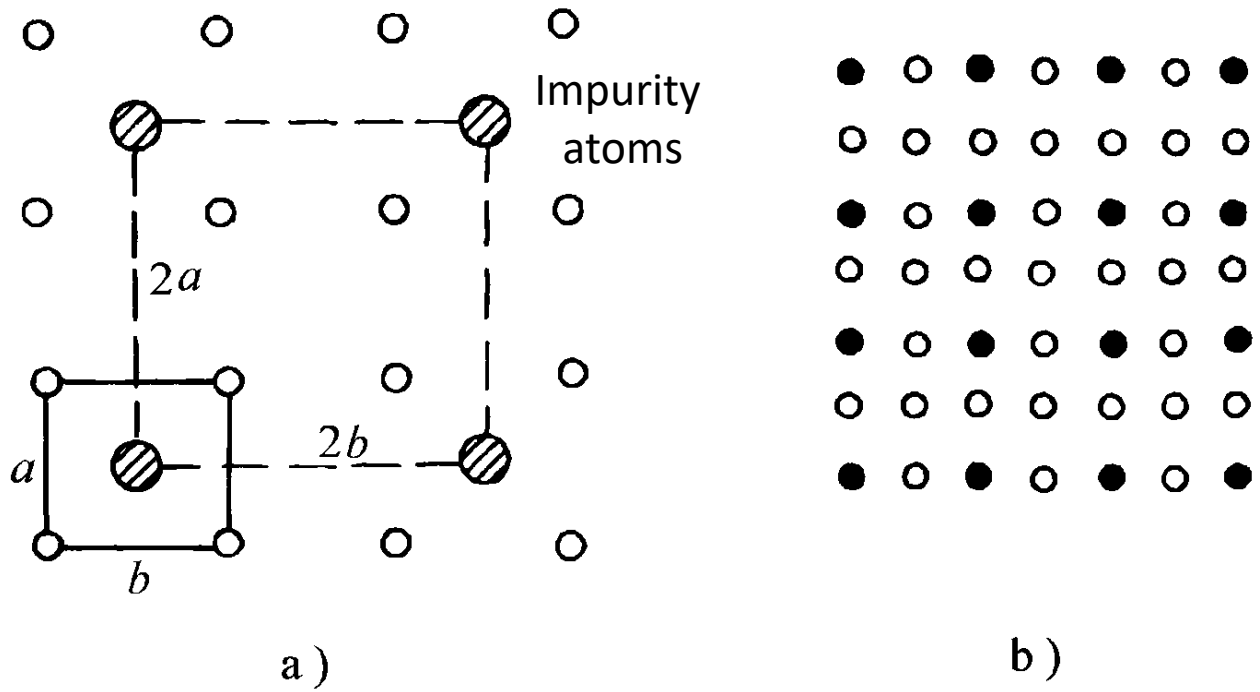

a) Two-dimensional lattice superstructure **b**) Reciprocal lattice

13.2 Low energy electron diffraction analysis

- Observation and recording of diffraction patterns

As shown in the figure, the electrons are accelerated, focused, and collimated by the three-stage focusing cup and are incident on the sample at the center of the hemispherical receiver. The grid G1 and the sample are grounded together to have an electric field-free space between them so that the low-energy electron beam does not produce distortion.

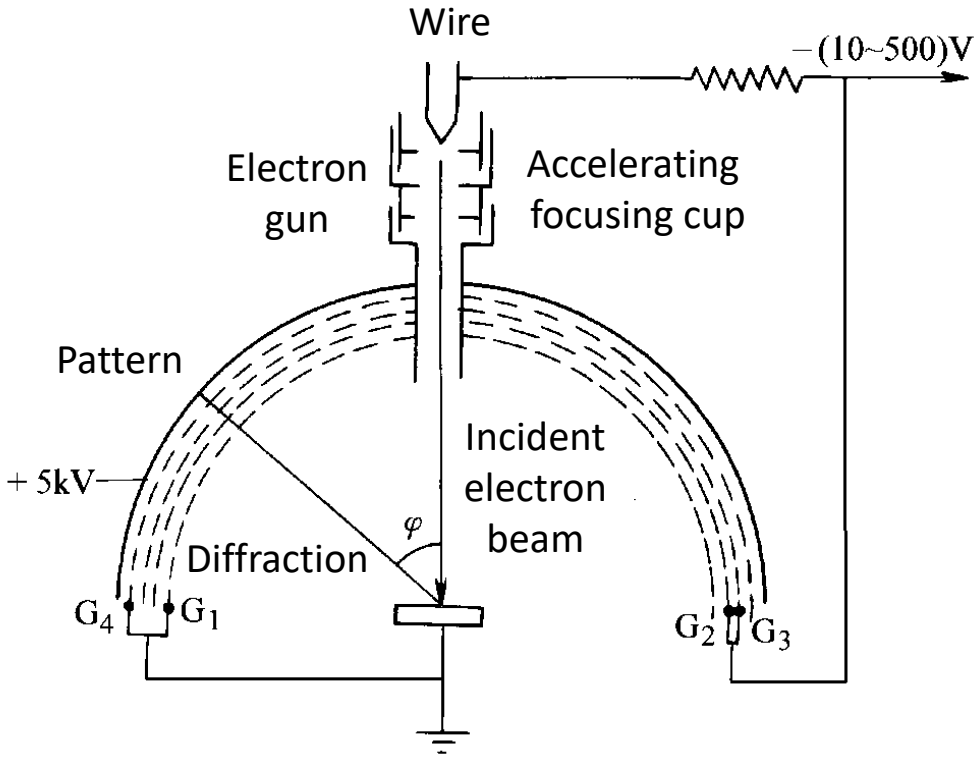

G2 and G3 are connected and have a slightly negative potential than the cathode to repel inelastically scattered electrons that lose energy; G4 is grounded to shield the receiving electrode.

Low-energy electrons are diffracted and then accelerated, called post-acceleration technology, which enhances weak information.

13.2 Low energy electron diffraction analysis

- Observation and recording of diffraction patterns

The figure shows the low-energy electron diffraction pattern of the (001) surface of **α-W** before and after the adsorption of oxygen atoms. We can see the impact of the adsorption of surface oxygen atoms on the surface structure.

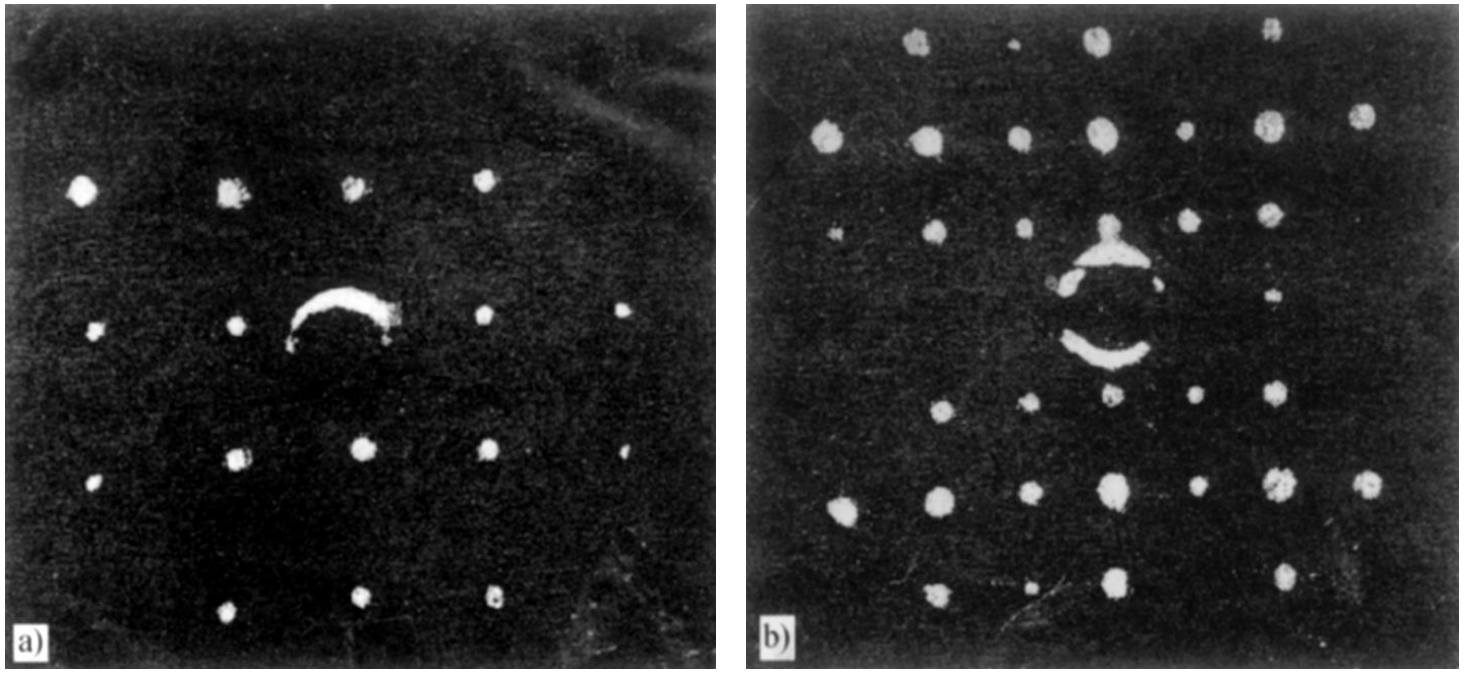

a) Clean the surface **b**) Adsorb oxygen atoms on the surface to form a superstructure

13.2 Low energy electron diffraction analysis

- Applications of low energy electron diffraction

Research on the atomic arrangement on the crystal surface found that metals such as Ni, Cu, W, Al, Cr, Nb, Ta, Fe, Mo, V, etc., have the same atomic arrangement in parallel crystal planes on the surface and in the inner layer; within a certain temperature range, Au, Pt, The surface structures of noble metals such as Pd and semiconductors Si and Ge are different from their internal structures of parallel crystal planes.

Research on the growth process of vapor deposition surface film: Explore the relationship between the surface film and the substrate structure, defects, and impurities, and study the growth process of the surface film.

Study on the formation mechanism of the oxide film. The formation of surface oxide film is a complex process: the adsorption of oxygen atoms, the reaction between oxygen and the surface, and the generation of three-dimensional oxides.

Research on gas adsorption and catalysis: For physical adsorption, a "two-dimensional phase change" occurs in the adsorption layer, that is, gas-liquid-crystal; many important results have been obtained on chemical adsorption and catalysis.

13.3 Auger electron spectroscopy analysis

- Auger transition and its probability

The Auger transition involves three extranuclear electrons. For an atom with atomic number ***Z***, the A shell electron is ionized, and the B shell electron transitions to the A shell, causing the C shell electron to be emitted. After that, the C shell energy is determined by $E_C(Z)$ changes to $E_C(Z+\Delta)$, so the characteristic energy $E_{ASC}(Z)$ of the Auger electron is:

$$E_{ASC}(Z) = E_A(Z) - E_B(Z) - E_C(Z+\Delta) - E_W$$

where Δ is a correction quantity, its value is 1/2 to 3/4, which can be approximately 1.

The outer layer electron transitions to the K-layer vacancy, which may release excess energy through the fluorescence or Auger effects. The relative emission probabilities of these two transition modes, the fluorescence yield ω_K, and the Auger electron yield $\overline{\alpha}_K$ satisfy:

$$\omega_K + \overline{\alpha}_K = 1$$

13.3 Auger electron spectroscopy analysis

- Auger transition and its probability

Common Auger electron energies correspond to the most likely transition processes. The Auger electron energies of various elements are shown in Figure 1.

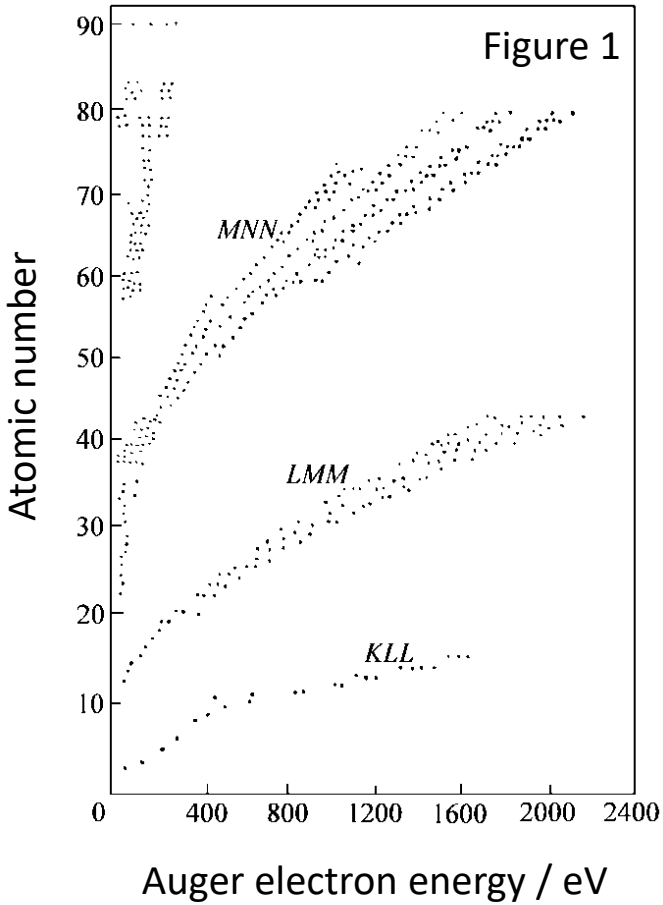

Figure 2 shows the effect of atomic number on the average Auger yield. The K series of elements with Z < 15, and the L and M series of almost all elements, are higher, and Auger electron spectroscopy analysis is more effective for light elements.

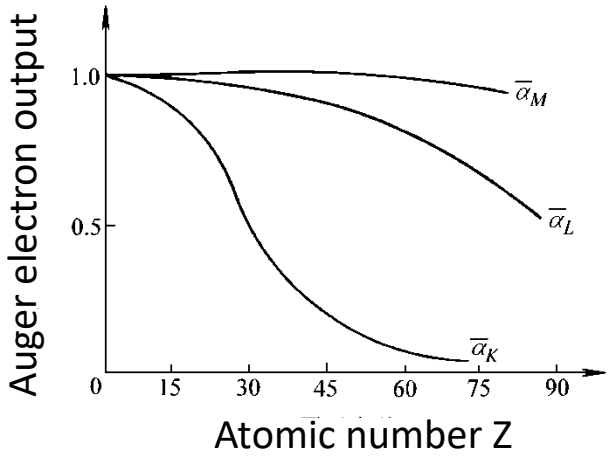

Figure 2

13.3 Auger electron spectroscopy analysis

- Detection of Auger electron spectroscopy

1) Blockage Analyzer

In a low-energy electron diffractometer (Figure 1), the electron gun acceleration voltage is increased and the grids G2 and G3 are at negative potential (-U) to block electrons with energy lower than eU, while electrons with energy higher than eU can reach the receiving electrode, which is called blocking analyzer.

Figure 1

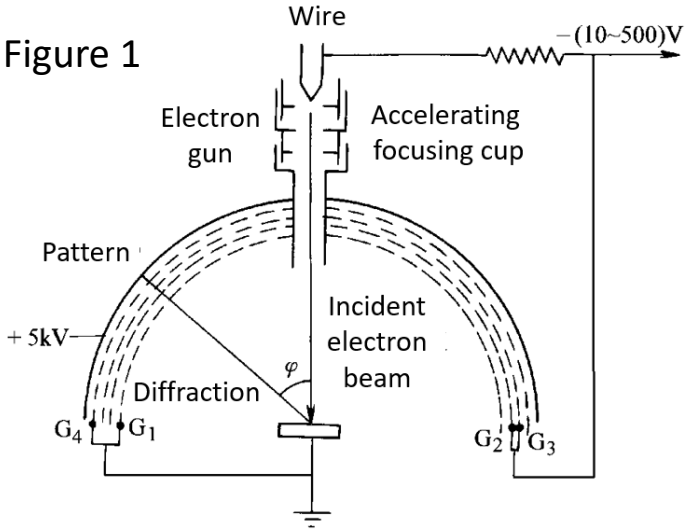

Figure 2

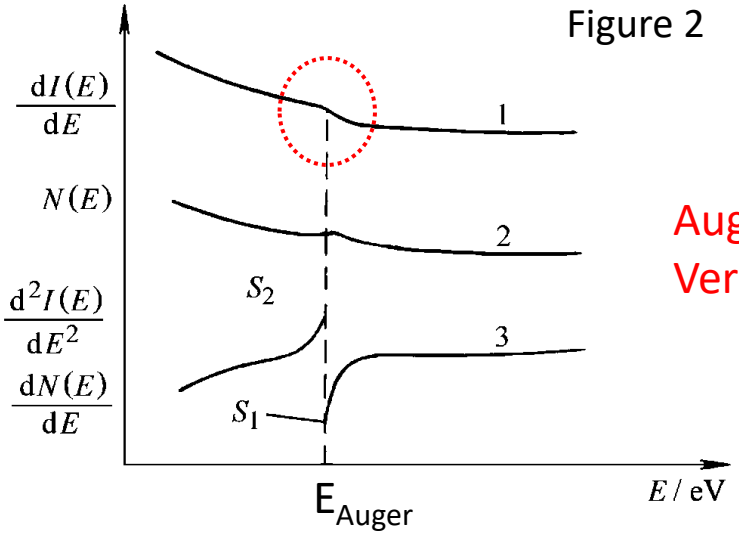

Auger Peak is weak
Very poor sensitivity

Figure 2 shows three display modes of received signal strength. Curve 1 shows the change of signal intensity I(E) with electron energy E.

13.3 Auger electron spectroscopy analysis

- Detection of Auger electron spectroscopy

1) Blockage Analyzer

To improve the sensitivity, an AC perturbation voltage $\Delta U = k\sin\omega t$ is superimposed on the DC blocking voltage. The signal strength $I(E + \Delta E)$ of the receiving pole has a slight amplitude modulation change. It is expanded by Taylor's formula, and when k is small, there is:

$$I = I_0 + I'k\sin\omega t + \frac{I''k^2}{4}\cos 2\omega t$$

Use a phase-sensitive detector to screen the ω or 2ω signal, rectify and amplify it, and give the change of $\frac{\mathrm{d}I(E)}{\mathrm{d}E}$ with E (curve 2); the change of $\frac{\mathrm{d}^2 I(E)}{\mathrm{d}E^2}$ with E (curve 3).

$$N(E) \propto \frac{\mathrm{d}I(E)}{\mathrm{d}E}$$

Curve 2 and 3's Auger peak is sharp and easy to distinguish, and is a commonly used display method.

13.3 Auger electron spectroscopy analysis

- Detection of Auger electron spectroscopy

2) Cylindrical Mirror Analyzer

The electrostatic reflection system consists of two coaxial cylindrical electrodes. The inner cylinder has an annular electron inlet ***E*** and an exit aperture B. The inner cylinder and the sample are grounded and the outer cylinder is connected to the deflection voltage ***U***, as shown in the figure.

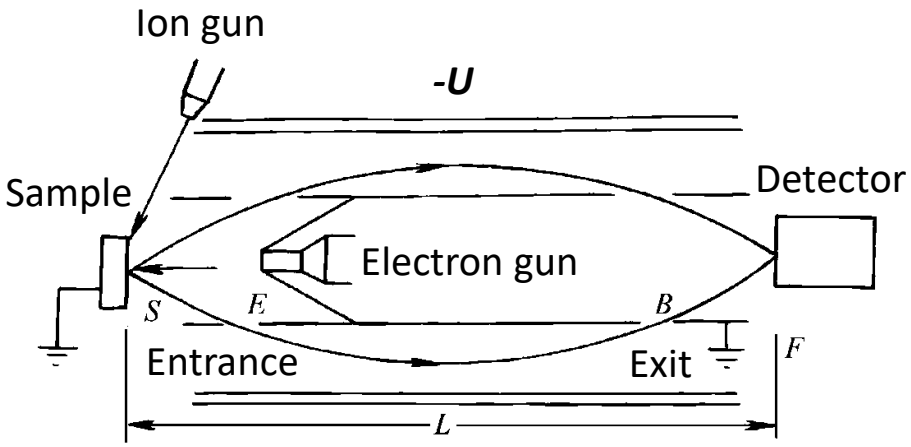

The radius of the two cylinders are r_1 and r_2 respectively, usually r_1 = 3 cm. If the aperture makes the electron emission angle ***42***°, the electrons with energy ***E*** emitted from point S on the sample will be focused at ***L*** = 6.19 from point S, and satisfies:

$$\frac{E}{eU} = 1.31 \ln \frac{r_1}{r_2}$$

By continuously changing the outer cylinder deflection voltage ***U***, the distribution curve of ***N(E)*** with ***E*** can be obtained, and the sensitivity can be improved by 2 to 3 orders of magnitude.

13.3 Auger electron spectroscopy analysis

- Detection of Auger electron spectroscopy

3) Quantitative analysis

The peak-to-peak amplitude S_1 S_2 of curve 3 symbolizes the element concentration in the effective excitation volume. To convert the peak-to-peak amplitude I_A of element A into the mole fraction C_A, pure elemental silver needs to be used as the standard sample, and the following is used Formula calculation:

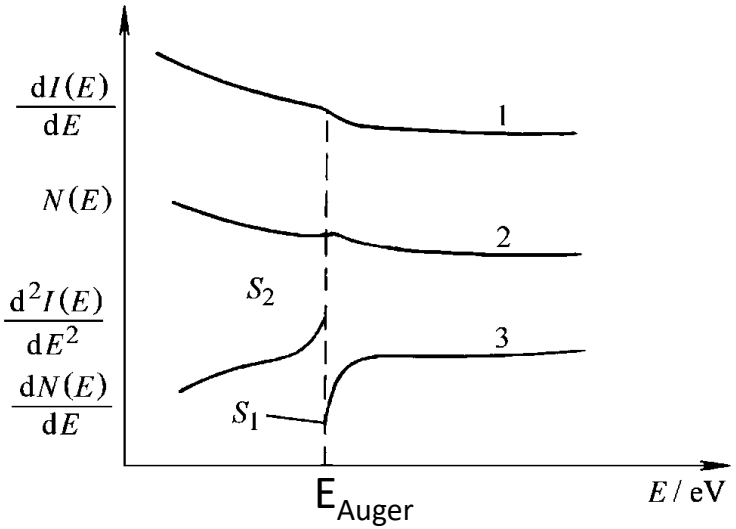

$$C_{\mathrm{A}} = \frac{I_{\mathrm{A}}}{I_{\mathrm{Ag}}^{0} S_{\mathrm{A}} D_X}$$

In the formula, I_{Ag}^{0} is the peak-to-peak amplitude of the pure silver standard sample; S_{A} is the relative Auger sensitivity factor of element A; D_X is the scaling factor. When the measurement conditions of I_{A} and I_{Ag}^{0} are the same, D_X = 1. If all elements (A , B , C ,..., N) have peak-peak amplitude, the calculation formula is:

$$C_{\mathrm{A}} = \frac{I_{\mathrm{A}} / S_{\mathrm{A}}}{\sum_{j=\mathrm{A}}^{N} (I_j / S_j)}$$

The analysis accuracy of Auger spectrometer is low and is generally considered to be semi-quantitative.

13.3 Auger electron spectroscopy analysis

- Application of Auger Electron Spectrometer

1) Surface segregation after pressure processing and heat treatment

After **18Cr9Ni** stainless steel was hot-rolled into 0.05 mm thin slices, Auger energy spectroscopy analysis found that the surface ***Ti*** concentration was much higher than its average composition; when it was subsequently heated to 1373 K, the surface ***Ti*** reached 40%; further heating to 1473 K, the ***Ti*** content decreased, and the ***S*** concentration Increases, ***O*** disappears, ***Ni***, ***P*** and ***Si*** appear.

The composition of the nickel-based alloy is **60Ni-20Co-10Cr-6Ti-4Al**. The original surface attachment elements include ***S***, ***Cl***, ***O***, ***C***, ***Na***, etc.; after vacuum heat treatment, the surface ***Al*** content increases significantly; after ion beam stripping of 30 nm, approximately The composition is Al_2O_3, which indicates that due to the low degree of vacuum during heat treatment, aluminum diffuses to the surface and oxygen forms alumina on the surface.

13.3 Auger electron spectroscopy analysis

- Application of Auger Electron Spectrometer

2) Grain boundary brittle fracture of metals and alloys

Alloy steel (0.39% ***C***, 3.5% ***Ni***, 1.6% ***Cr***, 0.06% ***Sb***) exhibits temper brittleness around 550°C. The grain boundary surface is obtained through low-temperature intergranular fracture, and its Auger electron spectrum is shown in the figure.

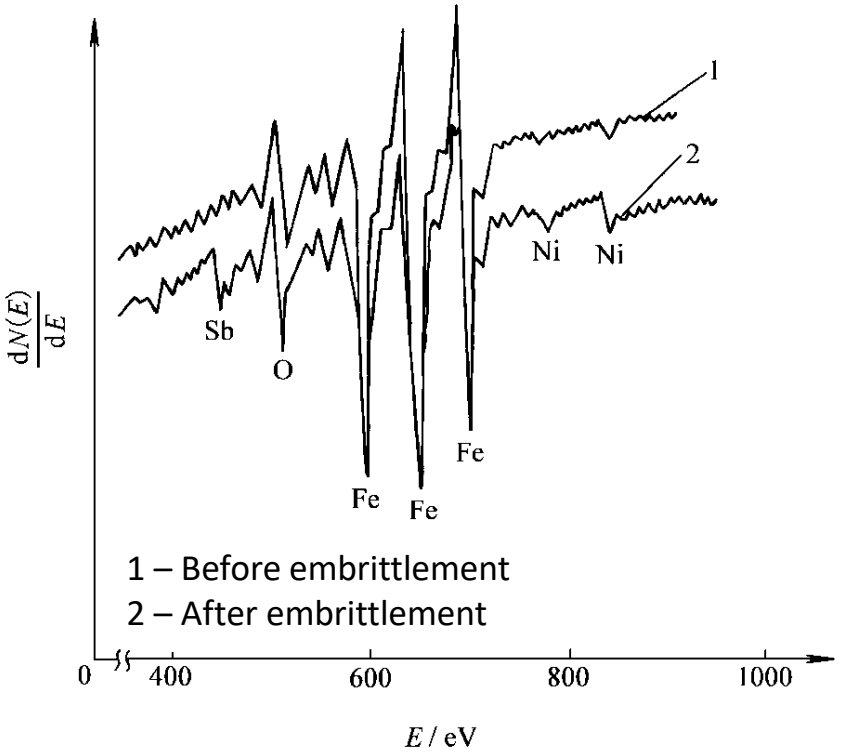

Comparing the spectral lines between the normal state and the tempered embrittlement state, it was found that the antimony concentration in the embrittled state was two orders of magnitude higher than the average composition; after 0.5 nm ion stripping, the antimony content dropped to the original average level, indicating the enrichment of antimony at the grain boundaries (only within a few atomic layers).

13.4 Field ion microscope and atom probe

- Structure of field ion microscope

The structure of a field ion microscope is shown in the figure. The sample is a single crystal filament with a tip radius of curvature of about 100 nm. It is connected to a high voltage of 10~40 kV as the anode, and the conductive layer on the inner wall of the glass container is grounded.

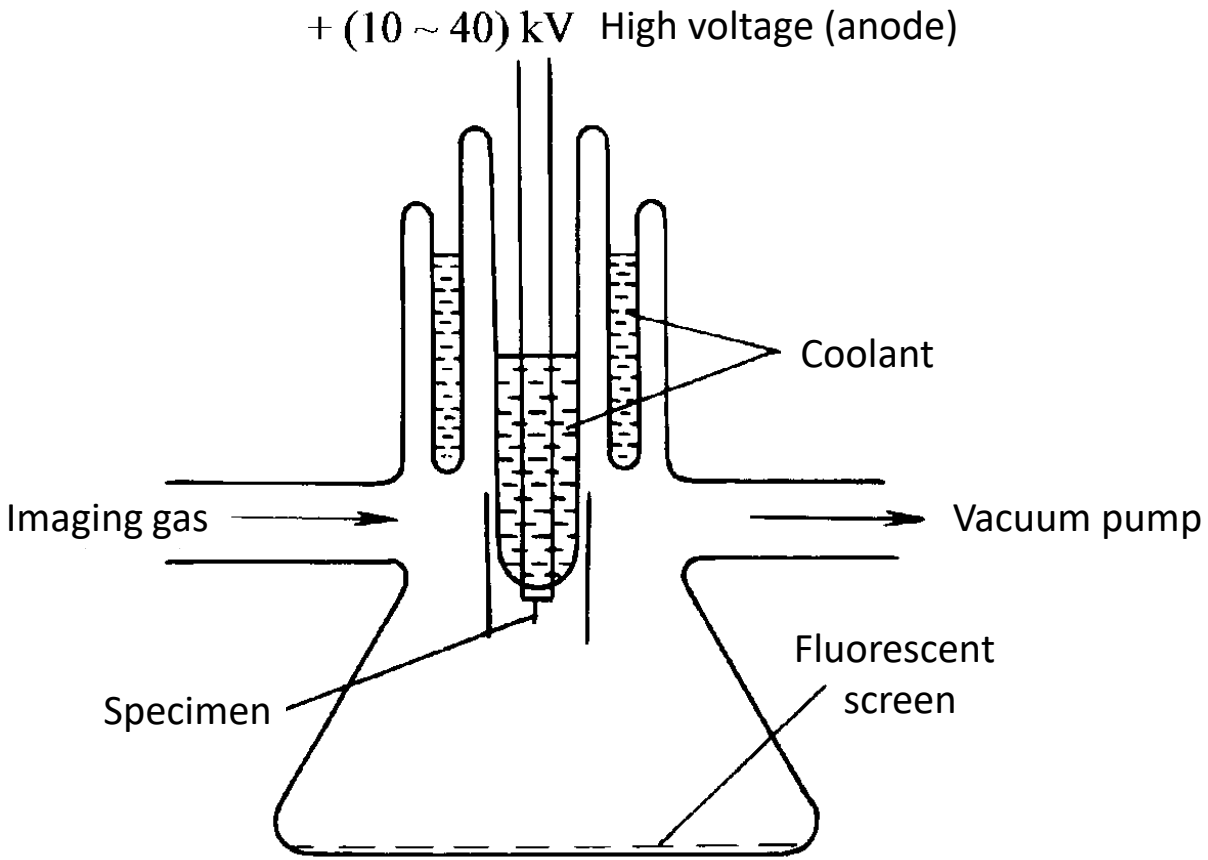

13.4 Field ion microscope and atom probe

- Structure of field ion microscope

When the instrument is working, first evacuate the container to 1.33×10^{-6} Pa, and then introduce imaging gas (such as helium) with a pressure of 1.33×10^{-1} Pa; when sufficient high pressure is applied to the sample, the gas atoms will be polarized and ionized, a clear image of the surface atoms at the tip is displayed on the fluorescent screen.

As shown in the figure, each bright spot is the image of a single atom.

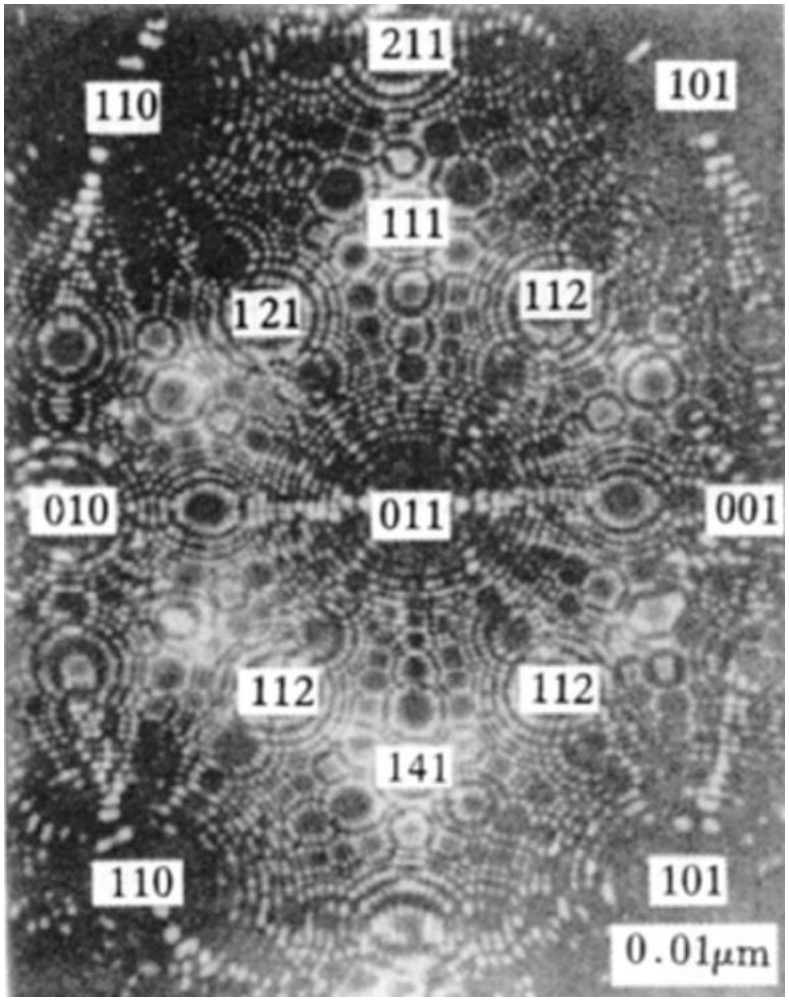

13.4 Field ion microscope and atom probe

- Field ionization and atomic imaging

If the sample voltage is U, the field intensity generated near its tip surface is the highest.

$$E \approx U/5r$$

As shown in the figure, when the imaging gas enters the container, the gas atoms are polarized under the action of extremely high potential gradient, and are accelerated by the electric field and hit the sample surface. They undergo several bounces on the surface and gradually lose their energy.

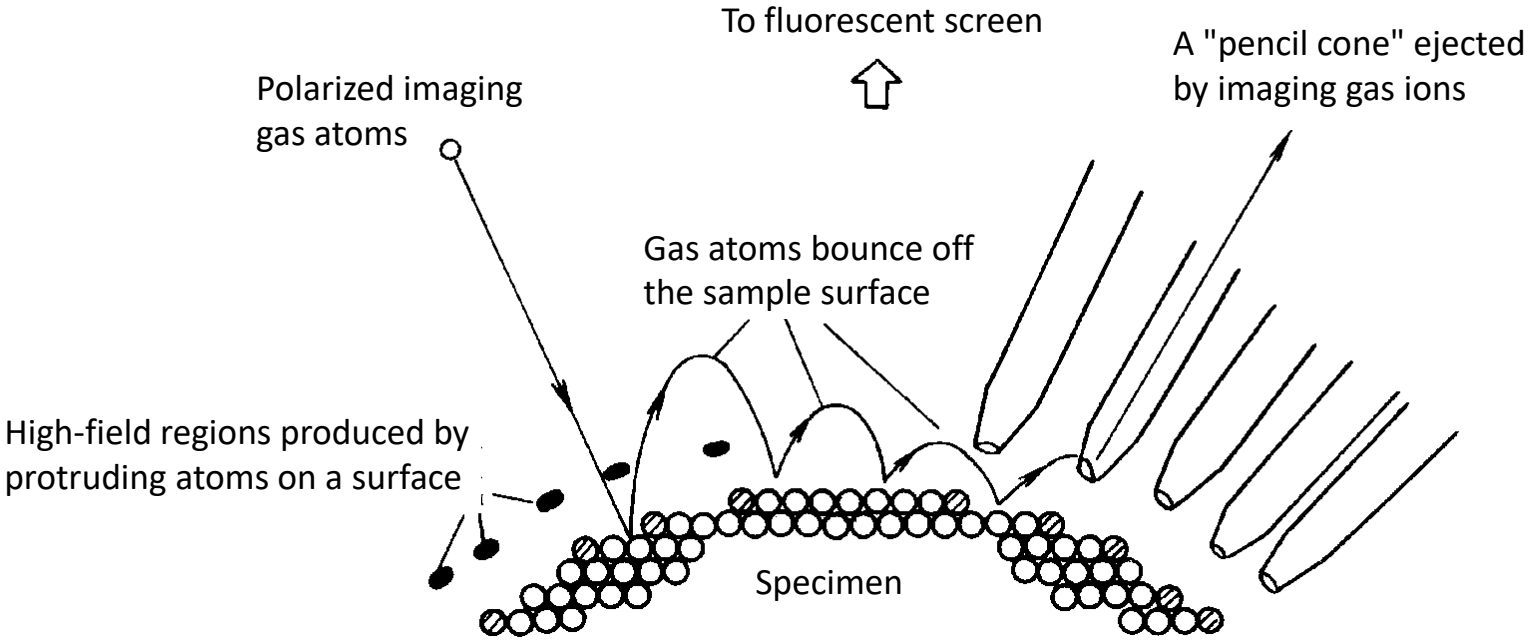

13.4 Field ion microscope and atom probe

- Field ionization and atomic imaging

Although the sample tip is approximately hemispherical, its surface is essentially composed of many atomic plane steps. The atoms at the edge of the steps protrude from the average hemispherical surface and have a smaller radius of curvature, so the field intensity near them is higher.

The polarized atoms in the high field strength area of protruding atoms are most easily ionized and are projected radially into the "pencil cone" of the observation screen. A large number of gas ions are collected, and bright spots appear on the observation screen. Each bright spot corresponds to a protruding atom on the sample's surface.

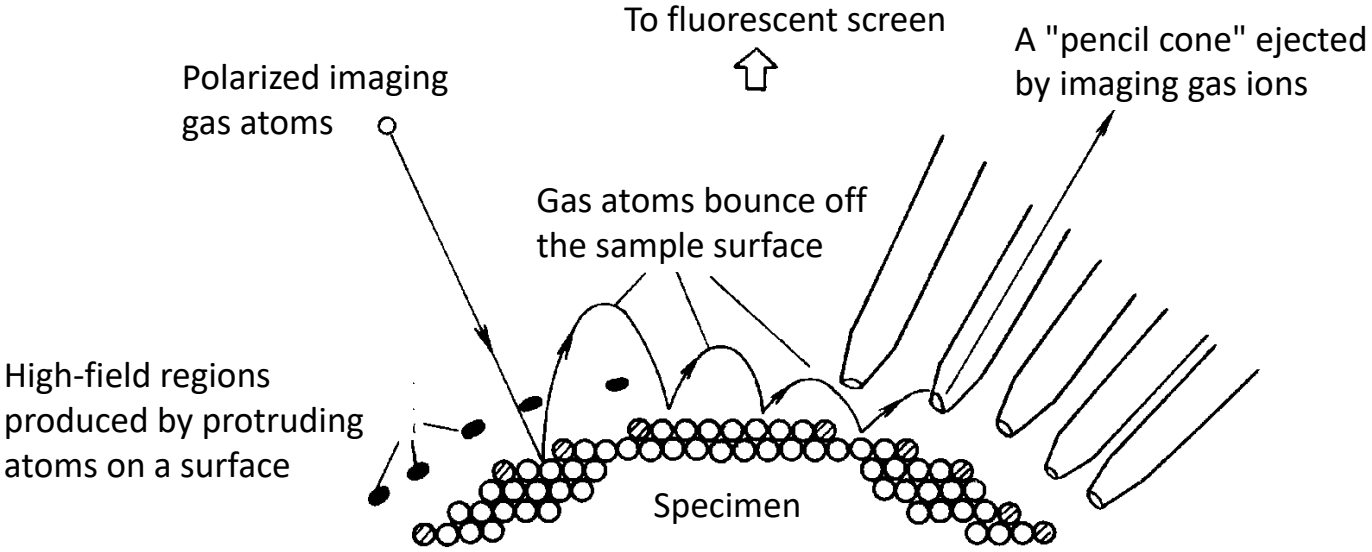

13.4 Field ion microscope and atom probe

- Field ionization and atomic imaging

The imaging field strength E_i required to ionize polarized gas mainly depends on the sample material, sample temperature, and the ionization excitation energy of the outer electrons of the imaging gas. The imaging field strengths of several gases are shown in the table.

Imaging field strengths of several gases

Imaging gas	He	Ne	H_2	Ar	Kr
E_i (MV/cm)	450	370	230	230	190

13.4 Field ion microscope and atom probe

- Interpretation of images

The field ion image consists of a large number of bright spot rings surrounding several centers. The same ring in the image corresponds to the image of protruding atoms at the edge of the same step; the center of the concentric ring is the radial projection pole of the normal line of the atomic plane, represented by its crystal plane index ,as the picture shows.

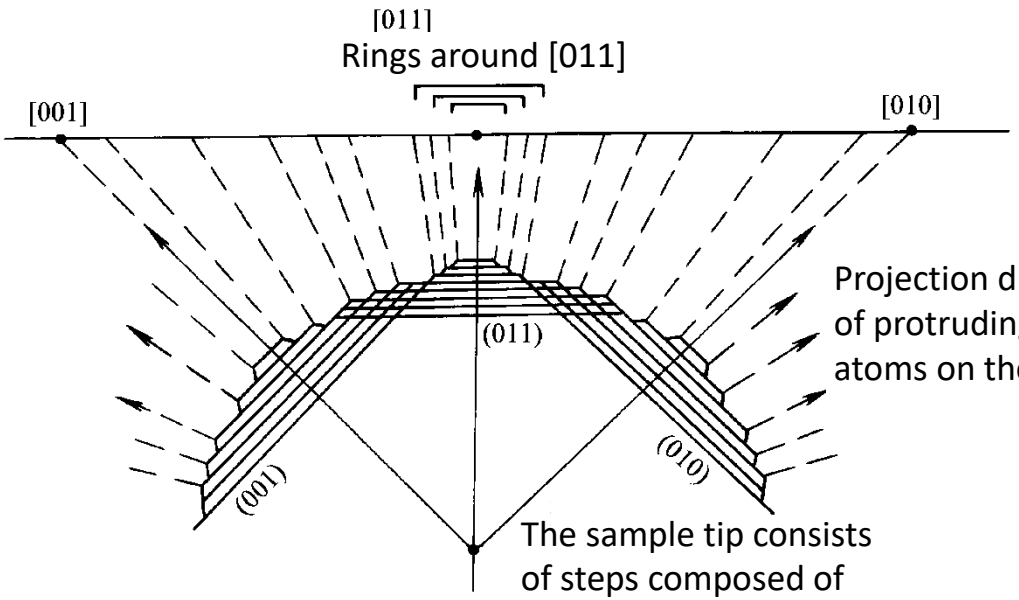

The field ion image can visually display the crystal symmetry, and can easily determine the sample orientation and the index. The field ion image magnification is:

$$M = R/r$$

In the formula, ***R*** is the distance from the sample to the observation screen, ***M*** can be as high as 10^6 times.

13.4 Field ion microscope and atom probe

- Field evaporation and delamination analysis

E_e is called the critical evaporation field strength, which mainly depends on certain physical parameters of the sample (such as bond strength) and temperature. When polarized gas atoms bounce on the sample surface, the sample atoms are evaporated as positive ions and ejected toward the fluorescent screen under an electric field. The evaporation field strengths of some metals are shown in the table.

Field evaporation can be used to purify the sample surface; field evaporation can be used for sample delamination analysis to reveal the three-dimensional structure of atomic arrangement.

In order to obtain a stable image, the sample needs to be kept cold, and the surface field strength must be kept below E_e but above E_i. This can be achieved by selecting the appropriate imaging gas and sample temperature.

The evaporation field strength of certain metals

Metal	Refractory metal	transition metals	Sn	Al
E_e (MV/cm)	400~500	300~400	220	160

13.4 Field ion microscope and atom probe

- Atom probe

Another application of field evaporation is the so-called "atom probe", which can be used to identify the elemental category of individual atoms on the surface of a sample. Its working principle is shown in the figure.

When a pulse high voltage ***U*** higher than the evaporation field intensity is applied to the sample, the evaporated ions pass through the small holes of the fluorescent screen and reach the ion detector. If the valence of the ion is ***n*** and the mass is ***m***, then its kinetic energy E_K is

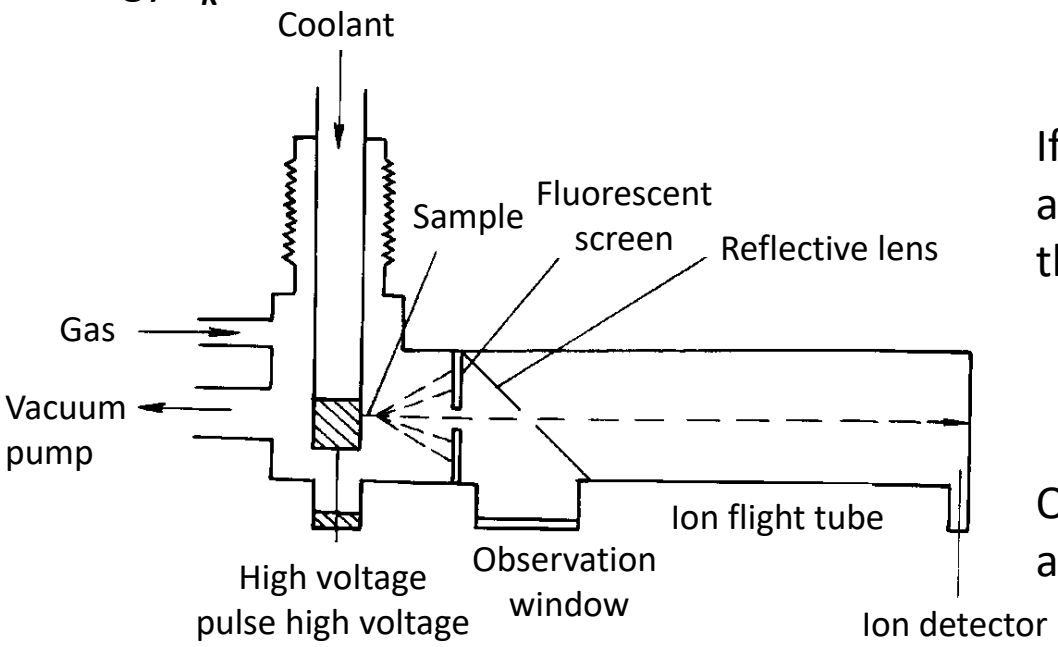

$$E_K = neU = \frac{1}{2}mv^2$$

If the flying time ***t*** can be measured and the distance from the sample to the detector is ***s***, then we have:

$$t \approx \frac{s}{v} = s/\sqrt{\frac{2neU}{m}}$$

Obtain compositional information at atomic resolution.

13.4 Field ion microscope and atom probe

- Applications of field ion microscopy

The main advantage of field ion microscopy is the direct imaging of surface atoms, but the number of atoms participating in the imaging is limited. In many theoretical studies of materials science, it is still a unique analysis method, and its main applications include:

1. Direct observation of point defects: vacancies or vacancy collections, gaps or replacement solute atoms in solid solutions, etc. Currently, only field ion microscopy can directly image them.
2. Dislocations: When dislocations emerge on the surface of a sample, field ion images directly reveal the atomic arrangement at the dislocation.
3. Interface defects: The study of interface atomic structure is one of field ion microscopy's earliest and most successful applications.
4. Early precipitation or ordering transformation of alloys: This analysis requires the identification of atomic categories, and the use of atom probes is a very suitable method.

13.4 Field ion microscope and atom probe

- Applications of field ion microscopy

As shown in the figure, the triangular mark is a dislocation outcrop, and the bright spots in the image form a spiral; while the image produced by the steps on the surface of an ideal crystal is a concentric ring.

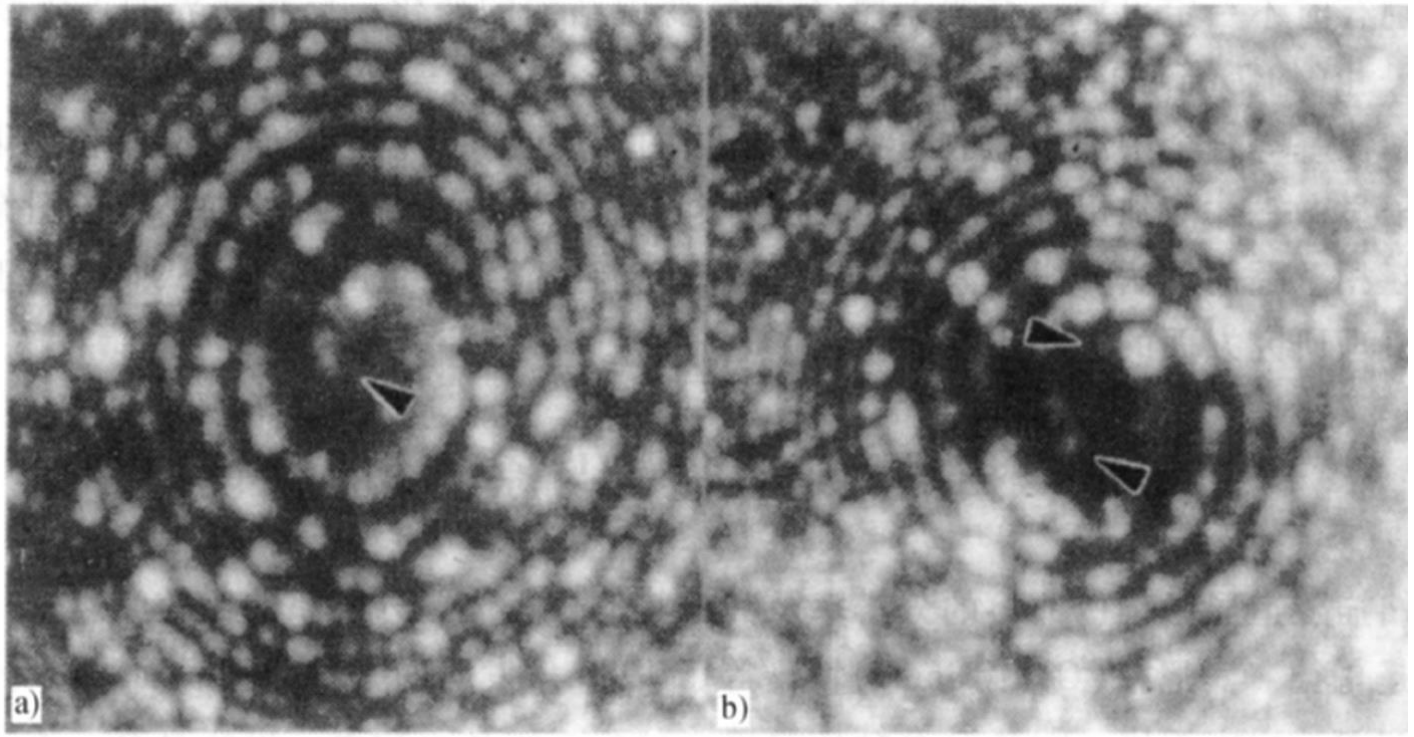

Field ion microscopy image of a sample containing dislocations
a) Single helix b) Double helix

13.4 Field ion microscope and atom probe

- Applications of field ion microscopy

As shown in the figure, the atoms on both sides of the grain boundary are very closely coordinated, and both sides are composed of single crystals with different orientations. The accuracy of displaying the atomic arrangement and orientation relationship on both sides of the grain boundary is approximately $\pm 2°$.

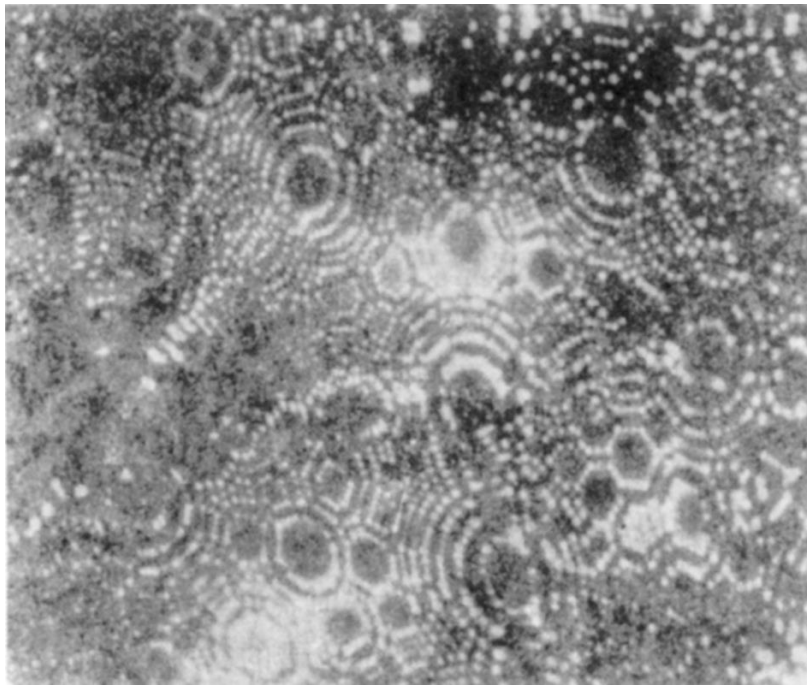

Field ion images of grain boundaries

13.5 Scanning Tunneling Microscope and Atomic Force Microscope

- Scanning Tunneling Microscope (STM)

As shown in the figure, A is the tip with atomic scale, and B is the sample to be analyzed. When STM works, a voltage is applied between the sample and the tip. When the distance between the sample and the tip is less than a certain value, a tunnel current is generated between the sample and the tip due to the quantum tunneling effect. It can be divided into constant current mode and constant height mode.

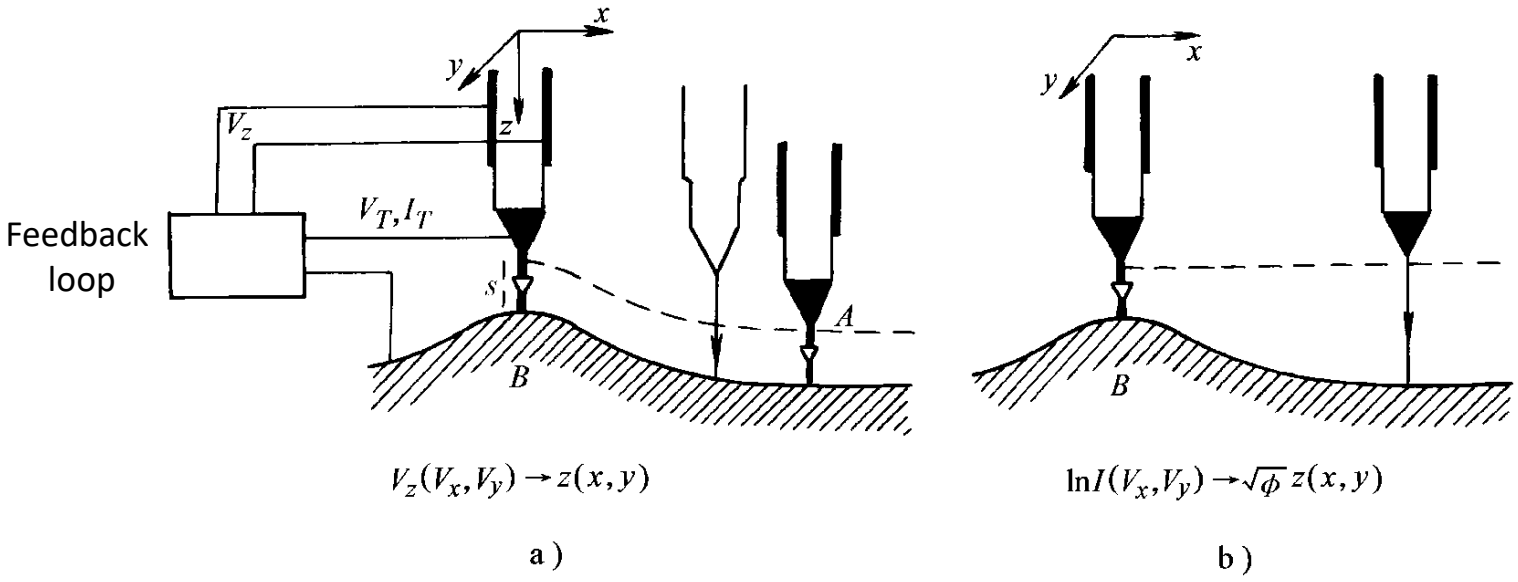

Schematic of the working principle of scanning tunneling microscope
a) Constant current mode **b**) Constant height mode

13.5 Scanning Tunneling Microscope and Atomic Force Microscope

- Scanning Tunneling Microscope (STM)

At low temperature and low pressure, the tunnel current ***I*** can be approximately expressed as:

$$I \propto \exp(-2kd)$$

In the formula, ***d*** is the distance between the sample and the tip; ***k*** is a constant, which can be approximately expressed as:

$$k = \frac{2\pi}{h}\sqrt{2m\Phi}$$

In the formula, ***m*** is the electron mass; Φ is the effective local work function; ***h*** is Planck's constant. The relationship between the tunnel current ***I***, the distance ***d*** between the sample and the tip and the average work function Φ is:

$$I \propto V_b \exp(-A\Phi^{1/2}d)$$

In the formula, V_b is the bias voltage between the tip and the sample; Φ is the average work function between the tip and the sample; ***A*** is a constant, which is approximately one under vacuum conditions. It can be seen from the calculation results that when the distance ***d*** decreases by 0.1 nm, the tunnel current I will increase by an order of magnitude.

13.5 Scanning Tunneling Microscope and Atomic Force Microscope

- Scanning Tunneling Microscope (STM)

The STM constant current mode is the most commonly used mode and is suitable for observing samples with large surface undulations; the constant height mode is suitable for observing samples with small surface undulations and can be used for fast scanning.

The figure shows the STM image of the surface reconstruction after CO adsorption on the Pt(111) surface.

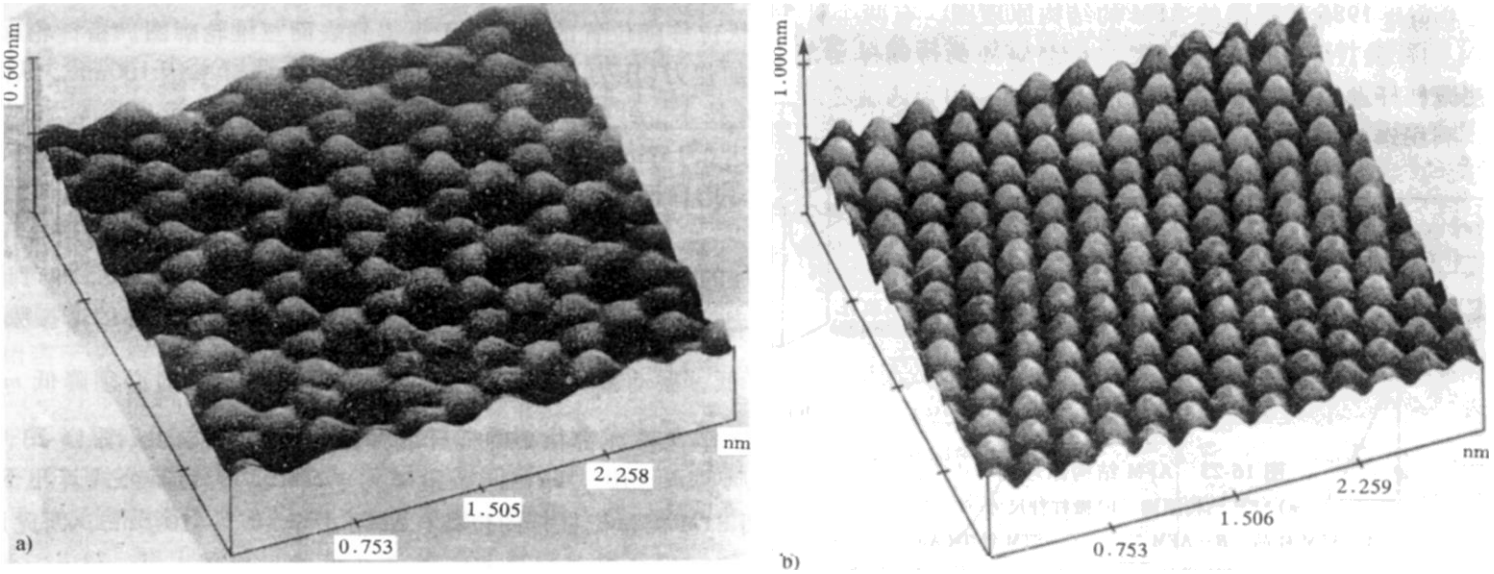

Reconstructed image after CO adsorption on Pt(111) surface
a) CO reconstructs the surface b CO transforms into CO2

13.5 Scanning Tunneling Microscope and Atomic Force Microscope

- Atomic Force Microscope (AFM)

Atomic force microscopy is suitable for measuring the surface morphology of conductive and insulating materials with a resolution close to the atomic scale. It can also measure the force between surface atoms and measure the elasticity, plasticity, hardness, adhesion, friction and other properties of the surface.

The structure and working principle of AFM are shown in the figure.

***A*-AFM sample**
***B*-AFM tip**
***C*-STM tip**
***D*-micro lever**
***E*- piezoelectric crystal**
***F*- fluoro rubber**

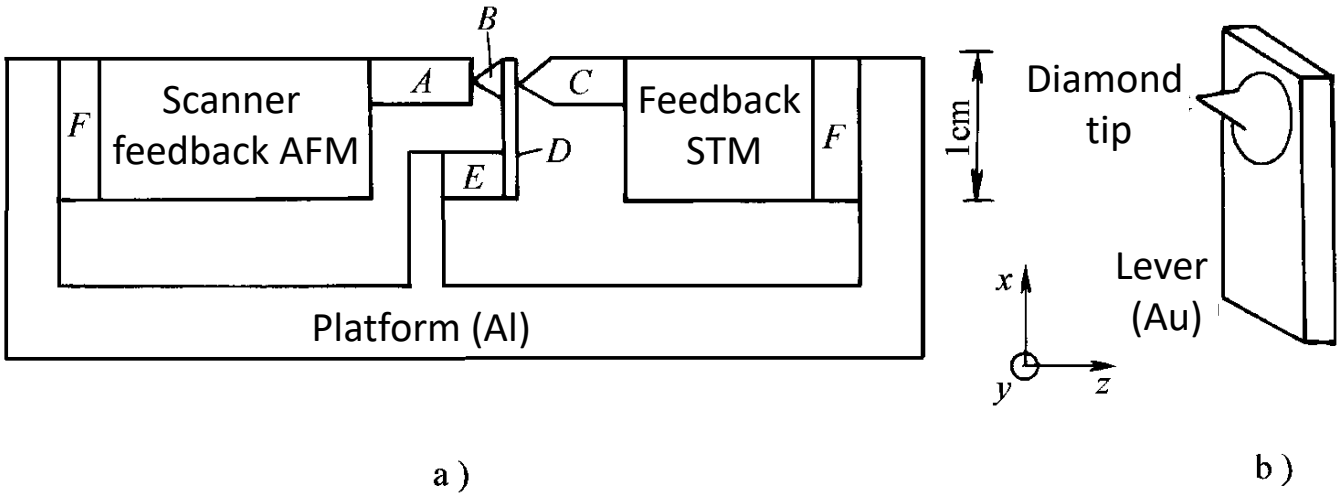

AFM structure schematic diagram
a) AFM structural principle b) Micro lever

13.5 Scanning Tunneling Microscope and Atomic Force Microscope

- Atomic Force Microscope (AFM)

The principle of AFM is close to that of pointer profilometer. Use the micro-lever **D** to gently press the needle tip **B** on the surface to be measured **A**. The needle tip and the surface to be measured move relative to each other, causing the needle tip to undulate with the surface unevenness. Use STM to measure the displacement Δz of the micro-lever, and you can obtain a three-dimensional profile of the surface.

Usually elastic elements or levers are used to measure the force ***F***, and there are:

$$F = S\Delta z$$

In the formula, ***S*** is the elastic coefficient. For AFM, Δz can be as small as 10^{-3}~10^{-5} nm, and the minimum force measured is 10^{-14}~10^{-16} N.

The AFM tip radius is close to the atomic size and measured in air with a lateral resolution of 0.15 nm and a longitudinal resolution of 0.05 nm.

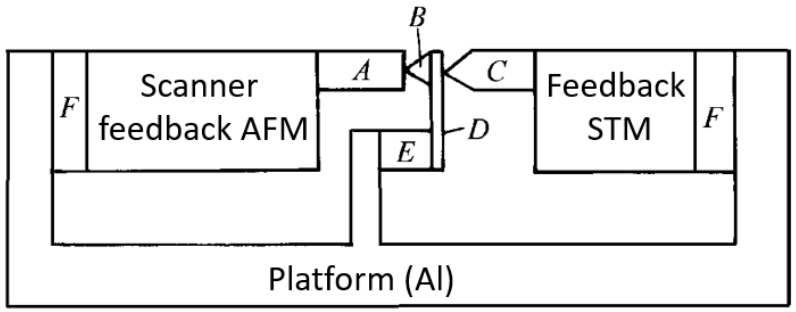

13.5 Scanning Tunneling Microscope and Atomic Force Microscope

- Atomic Force Microscope (AFM)

When the distance is far from the sample surface, the surface force is negative (attractive force). As the distance decreases, the attractive force first increases and then decreases until it is zero; when the distance further decreases, the surface force becomes positive (repulsive force), and the surface force increases rapidly as the distance further decreases.

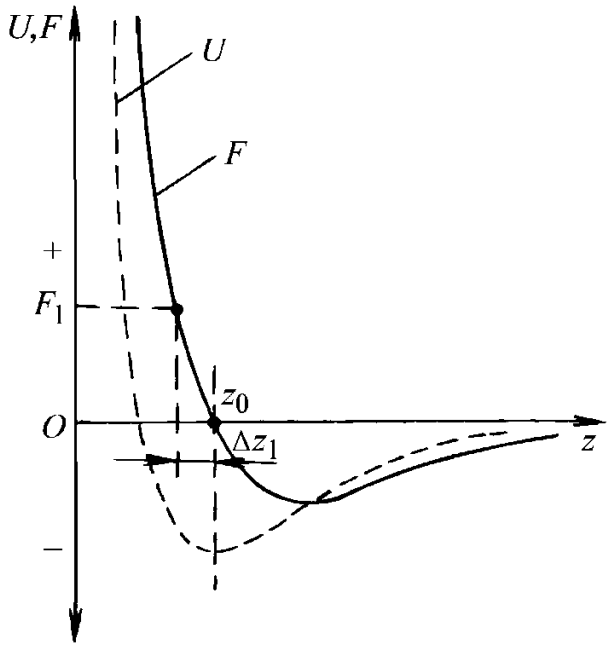

The distance between sample A and tip B is determined by the voltage applied by **Pz** of AFM and STM (piezoelectric ceramic that controls z-direction displacement); the size and direction of the surface force are determined by the change of voltage applied by **Pz** of STM.

The variation curve of the sample surface force with distance felt by the top atoms of tip B can be obtained from this.

Curves of sample surface potential energy ***U*** and surface force ***F*** changing with surface distance ***z***.

13.5 Scanning Tunneling Microscope and Atomic Force Microscope

- Atomic Force Microscope (AFM)

If the hardness of tip B is very high, measure the elastic deformation or plastic deformation of the AFM sample as a function of force. For ideal elastic materials, the change of ***F*** with the depth of the needle tip entering the sample is shown in Figure **a**. When the sample retracts, ***F*** decreases to zero along the original curve; for ideal plastic materials, after the needle tip enters the depth of the sample, the sample retracts slightly, ***F*** immediately drops to zero. See Figure **b**.

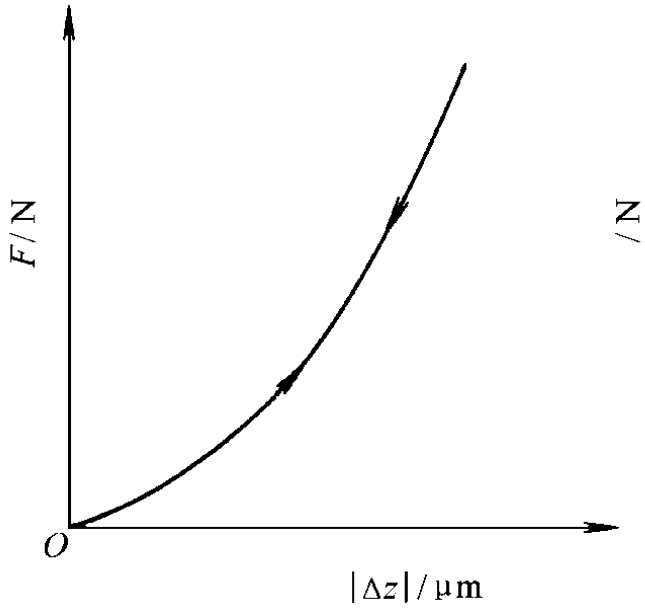

a)

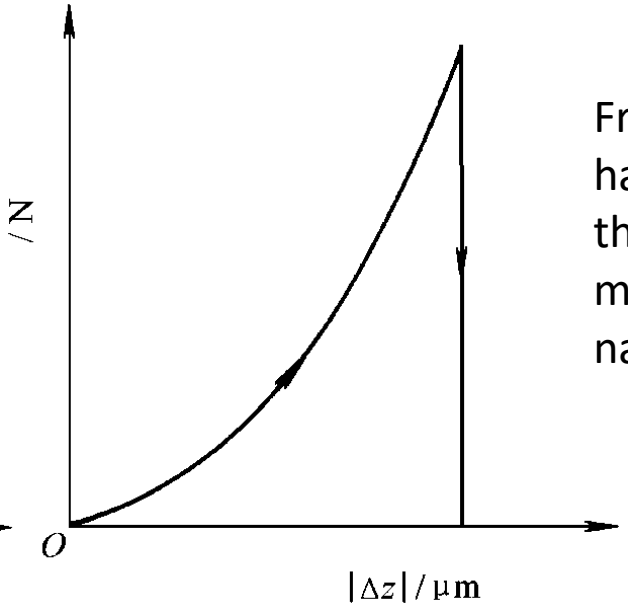

b)

From this, the elasticity, hardness, plasticity, etc., of the material can be measured, that is, the nanoindentation method.

13.6 X-ray photoelectron spectroscopy analysis

- Measurement principle of X-ray photoelectron spectroscopy

The measurement principle of X-ray photoelectron spectroscopy is based on the law of photoelectric emission. For an isolated atom, its photoelectron kinetic energy E_k is

$$E_k = h\nu - E_b$$

In the formula, $h\nu$ is the incident photon energy; E_b is the electron binding energy.

Different energy levels of the same atom correspond to different E_b, so the same element will have photoelectrons of different energies. When an energy analyzer is used to analyze the kinetic energy of photoelectrons emitted by a solid sample, the kinetic energy of the photoelectrons entering the analyzer is:

$$E_k' = h\nu - E_b - \varphi_s - (\varphi_A - \varphi_s) = h\nu - E_b - \varphi_A$$

In the formula, φ_s is the work function of the sample; φ_A is the work function of the analyzer material.

If $h\nu$ and φ_A are known, and E_k' is measured by the energy analyzer, E_b can be calculated using the formula, and surface composition analysis can be carried out.

13.6 X-ray photoelectron spectroscopy analysis

- Measurement principle of X-ray photoelectron spectroscopy

In X-ray photoelectron energy spectrum, the electron energy level symbol is represented by nl_j. For example, the energy level of $n = 2$, $l = 1$ (i.e. p electron), $j = 3/2$ is expressed as $2p_{3/2}$; $1s_{1/2}$ is generally written as **1s**.

The $2p_{3/2}$ photoelectron energy is shown in the figure, which can clearly express the relationship between the energies in the formula.

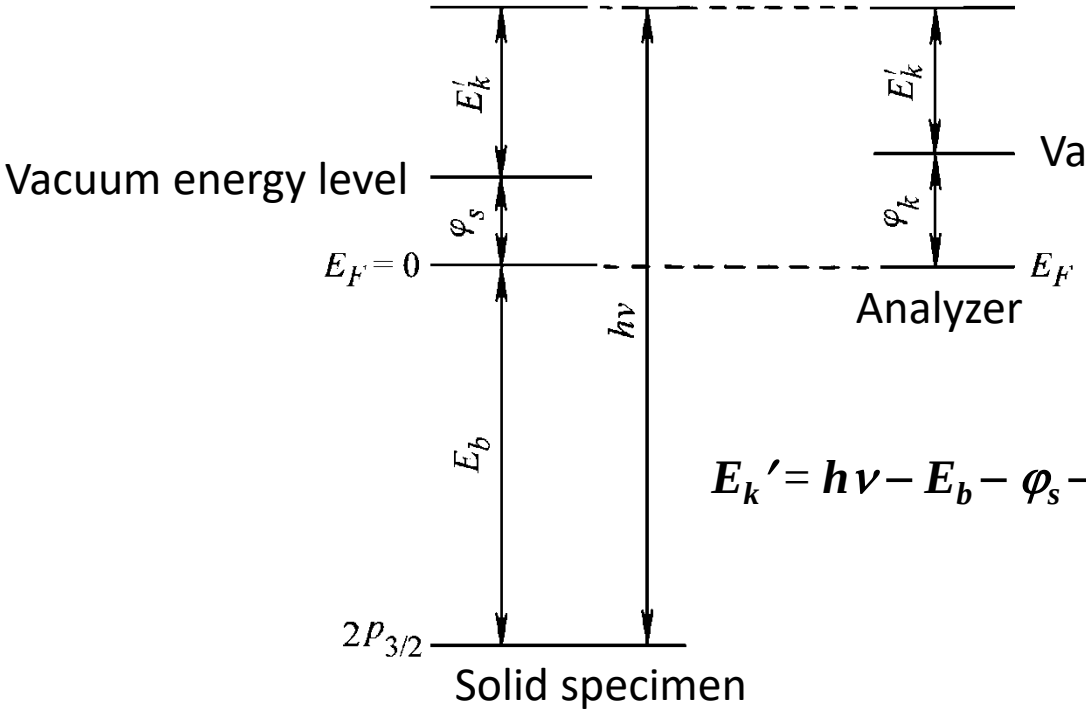

$$E_k' = h\nu - E_b - \varphi_s - (\varphi_A - \varphi_s) = h\nu - E_b - \varphi_A$$

13.6 X-ray photoelectron spectroscopy analysis

- Measurement principle of X-ray photoelectron spectroscopy

The picture shows the diagram of the X-ray photoelectron spectrometer. There are two commonly used X-ray sources, one is the K_α of Mg, and the other is the K_α of Al. The line widths are 0.7 eV and 0.9 eV respectively. Monochromators can be used to reduce the linewidth of X-ray sources.

The energy analyzer is mainly a hemispheric or nearly hemispheric ball deflection analyzer SDA, followed by a dual-channel tube mirror analyzer CMA. By controlling a certain voltage of the analyzer, the selected photoelectron energy can be controlled; if a scanning voltage is used, the photoelectron energy spectrum can be obtained.

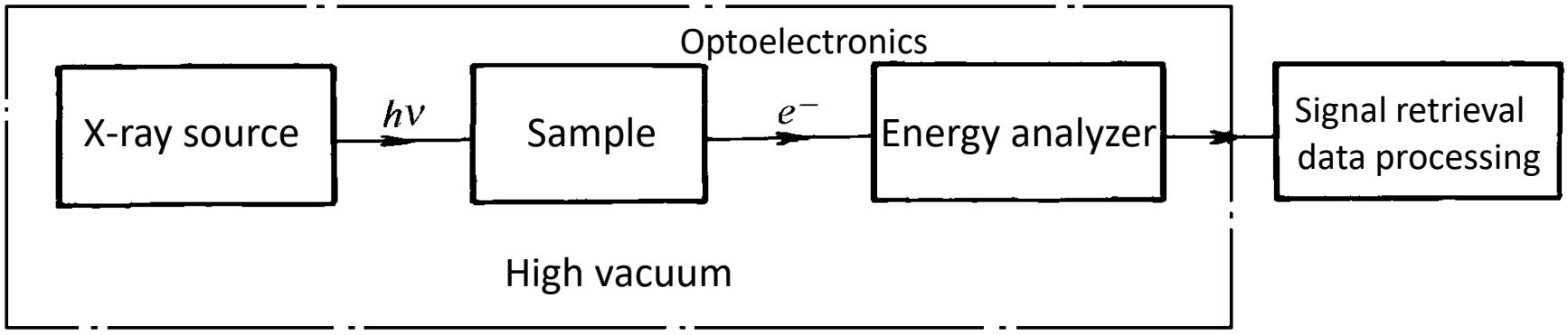

X-ray photoelectron spectrometer principle block diagram

13.6 X-ray photoelectron spectroscopy analysis

- Measurement principle of X-ray photoelectron spectroscopy

The figure below shows the X-ray photoelectron spectrum of copper-nickel alloy. Experimental conditions: beam spot size 500 μm; spectrum collection time 10s.

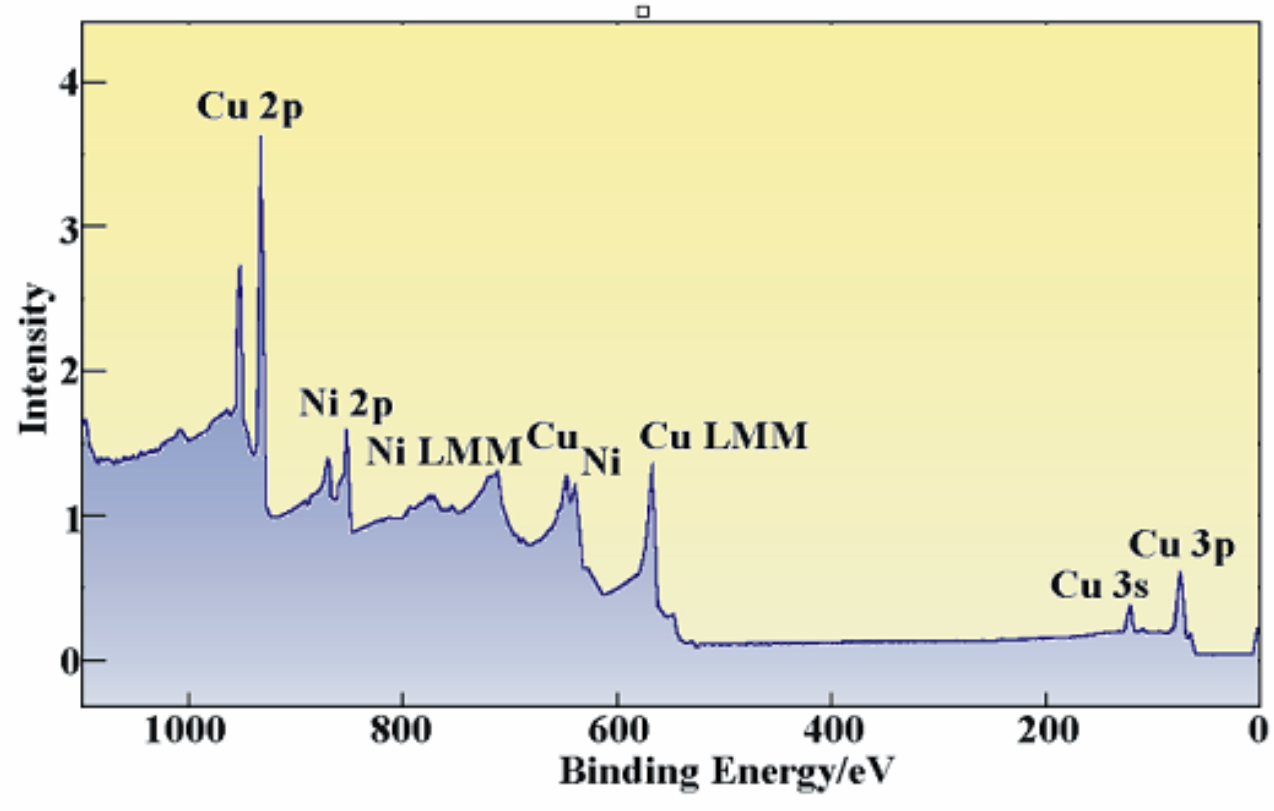

X-ray photoelectron spectrum of copper-nickel alloy

13.6 X-ray photoelectron spectroscopy analysis

- Qualitative analysis

X-ray photoelectron spectroscopy can obtain rich chemical information. According to the photoelectron spectrum's peak position (energy), the types of elements present in the sample analysis area can be determined; chemical shift data can be used to determine the chemical state of the elements present. This is a qualitative analysis, which can be carried out with the help of relevant manuals.

Generally, when performing qualitative analysis, first scan the entire range of X-ray photoelectron energy to identify all elements present; then scan the selected peaks in a small range to identify their chemical state.

If X-ray photoelectron spectroscopy is combined with ion sputter surface etching, a depth distribution of elements and their chemical states can be obtained.

If there are Auger peaks in the spectrum, fully use the chemical information they carry.

13.7 Infrared Spectrum

- Overview of infrared spectroscopy
- In 1800, it was first discovered that in addition to the red light of the visible spectrum, there was an invisible extended spectrum with obvious thermal effects.
- In 1887, infrared rays were successfully generated in the laboratory, leading to the realization that infrared rays are essentially the same as visible light and radio waves.
- In 1889, it was first confirmed that CO and CO_2 have different infrared spectra. This shows that the source of infrared absorption is molecules rather than atoms. This is the basis for establishing the discipline of molecular spectroscopy.
- In the 20th century, due to the needs of production practice, the development of various new technologies was promoted. Infrared science also came out of the laboratory and began to be applied to production, forming a brand-new technology - infrared technology.

13.7 Infrared Spectrum

- Infrared spectrum classification

- According to wavelength range:

1) The near-infrared band spectrum is 1~3 μm, which is generated by frequency doubling and combined frequency of molecules.
2) The mid-infrared band spectrum is 3~40 μm, which belongs to the fundamental frequency vibration spectrum of molecules.
3) The far-infrared band spectrum is 40~1000 μm, which belongs to the rotation spectrum of molecules and the vibration spectrum of certain groups.

The mid-infrared region is the most studied and applied band.

- According to the production method:

1) The absorption spectrum depends on the composition and structure of the material molecules.
2) The emission spectrum depends on the temperature and chemical composition of the object.

Absorption spectroscopy is a commonly used and main method.

13.7 Infrared Spectrum

- Development and types of infrared spectrometers

The research and development of infrared spectrometers has gone through the following stages:

1) In 1908, an infrared spectrometer using sodium chloride crystal as a prism was developed.
2) In 1910, the Echelle grating infrared spectrometer was developed.
3) In 1918, a high-resolution infrared spectrometer was developed
4) In the 1940s, the development of a double-beam infrared spectrometer began
5) In 1950, double-beam infrared spectroscopy entered commercialization
6) Modern infrared spectroscopy is based on the Fourier transform. An interferometer is used to obtain an interference pattern. Fourier transform is used to convert the interference pattern with time as a variable into a spectrum with frequency as a variable.

13.7 Infrared Spectrum

- Development and types of infrared spectrometers

Absorption spectroscopy is mainly used to study infrared spectroscopy, which can be divided into two types:

1) Dispersive spectrometer

Use a prism or grating as a monochromator and use single-channel or multi-channel measurement to obtain the spectral distribution of the source.

2) Non-dispersive spectrometer

Also called Fourier transform infrared spectrometer, its core part is a double-beam interferometer, commonly used Michelson interferometer. When the moving mirror in the instrument moves, the optical path difference between the two coherent beams passing through the interferometer changes, and the light intensity measured by the detector also changes accordingly, thereby obtaining an interference pattern.

13.7 Infrared Spectrum

- Development and types of infrared spectrometers

2) Non-dispersive spectrometer

The period of the interference light is $\lambda/2$, and its intensity is $I(x)$, which is related to the optical path difference x.

$$I(x) = B(v)\cos(2\pi vx)$$

In the formula, $B(v)$ is the intensity of incident light and is a function of the frequency of incident light.

The above formula represents the intensity of monochromatic light of a certain frequency v. By integrating the above formula, the total interference light intensity of the superposition of monochromatic light of various frequencies can be obtained.

$$I(x) = \int_{-\infty}^{\infty} B(v)\cos(2\pi vx)\mathrm{d}v$$

After Fourier transformation, the spectrum of the incident light can be obtained, that is, the change of intensity with frequency.

$$B(v) = \int_{-\infty}^{\infty} I(x)\cos(2\pi vx)\mathrm{d}x$$

13.7 Infrared Spectrum

- Development and types of infrared spectrometers

2) Non-dispersive spectrometer

The working principle of the Fourier transform infrared spectrometer is shown in the figure. It is mainly composed of light source, interferometer, computer system, etc. The core part is the Michelson interferometer.

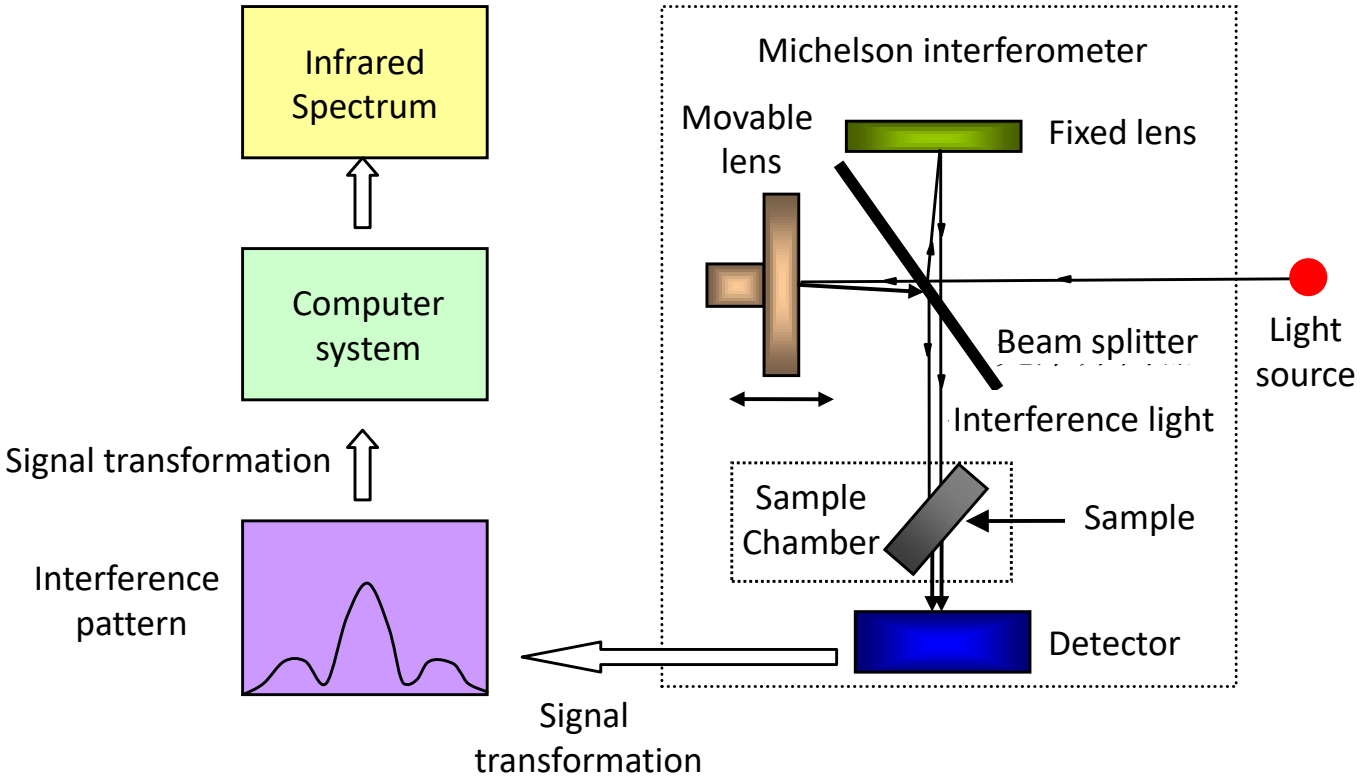

13.7 Infrared Spectrum

- Development and types of infrared spectrometers

2) Non-dispersive spectrometer

The infrared light source enters the interferometer after being collimated and parallel; it is modulated into a beam of interference light and passes through the sample; an interference signal containing spectral information is obtained and reaches the detector; the interference signal is converted into an electrical signal and an interference pattern is drawn; the interference pattern is then sent through signal conversion Use a computer to perform Fourier transform to obtain the infrared spectrum with wave number as the abscissa.

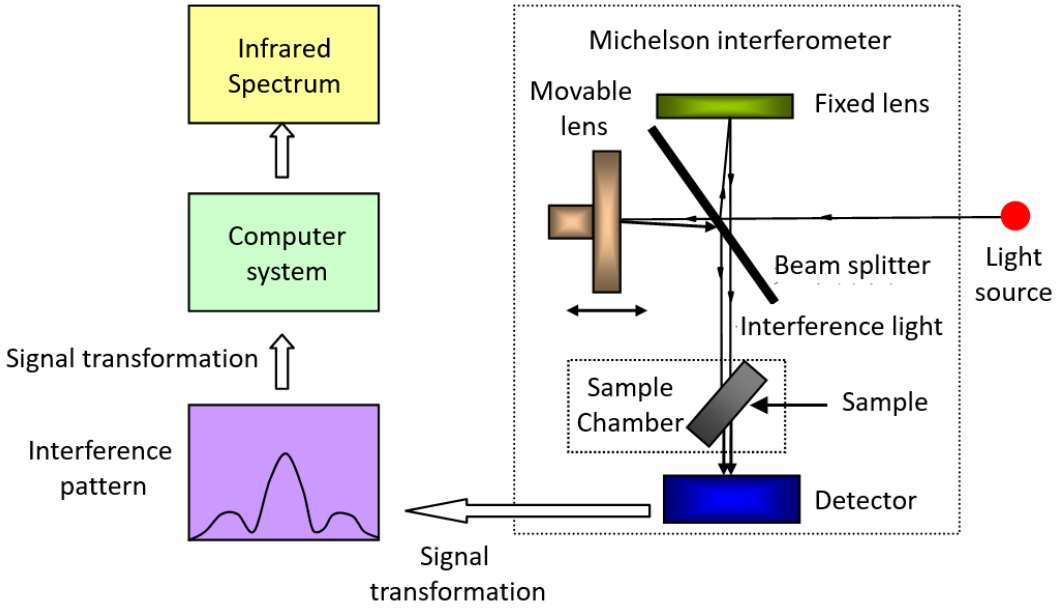

13.7 Infrared Spectrum

- Development and types of infrared spectrometers

2) Non-dispersive spectrometer

Advantages of Fourier transform infrared spectrometer: multi-channel measurement, high signal-to-noise ratio; high luminous flux, high sensitivity; wave value accuracy can reach 0.01 cm^{-1}; increasing the moving distance of the moving mirror can improve the resolution; the working band can be extended from the visible region to the millimeter region, enabling measurement of far-infrared spectra.

13.7 Infrared Spectrum

- Infrared Spectroscopy and Molecular Vibrations

The infrared spectrum is closely related to molecular vibration. Molecular vibration can be explained by diatomic vibration. Diatomic vibration includes two models: harmonic oscillator and anharmonic oscillator. As shown in the figure, the resonator vibration model treats two atoms as small balls with masses m_1 and m_2, making simple harmonic vibrations in the direction of their bond axes, so the diatomic molecule is called a resonator. According to Hooke's law, the vibration wave number can be obtained ν'.

$$\nu' = \frac{1}{2\pi c}\sqrt{\frac{k}{\mu}}$$

In the formula, ***c*** is the speed of light; ***k*** is the force constant of the chemical bond; **μ** is the reduced mass.

$$\mu = \frac{m_1 m_2}{m_1 + m_2}$$

Compression
Displacement: **-*x***

Balance
Displacement: **0**

Extension
Displacement: **x**

13.7 Infrared Spectrum

- Infrared Spectroscopy and Molecular Vibrations

According to quantum mechanics, the solution to the Schrödinger equation for this system is:

$$E = \left(v + \frac{1}{2}\right)\frac{h}{2\pi c}\sqrt{\frac{k}{\mu}}$$

In the formula, ***v*** = 0, 1, 2, 3... are called vibration quantum numbers. Its potential energy function is a symmetrical parabola, as shown in figure a.

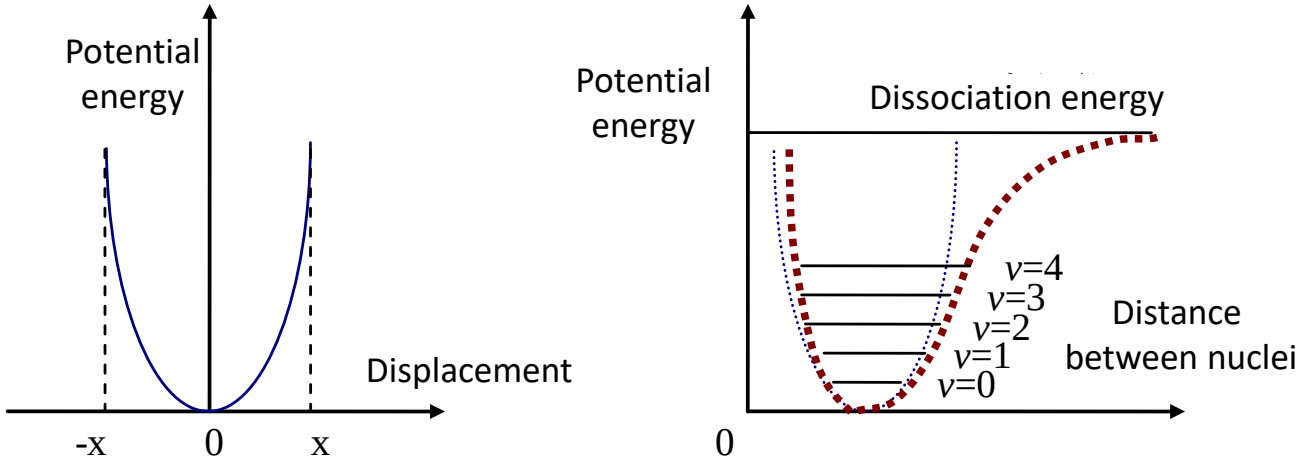

Harmonic oscillator **a**) and non-harmonic oscillator **b**) potential energy function

13.7 Infrared Spectrum

- Infrared Spectroscopy and Molecular Vibrations

In fact, the diatomic molecule is not an ideal harmonic oscillator. Its potential energy function is no longer a symmetrical parabola, but a curve as shown in Figure b. The actual potential energy of the molecule increases as the distance between the nuclei increases. When the distance between the nuclei increases, When reaching a certain level, the molecules will dissociate into atoms. At this time, the potential energy is a constant.

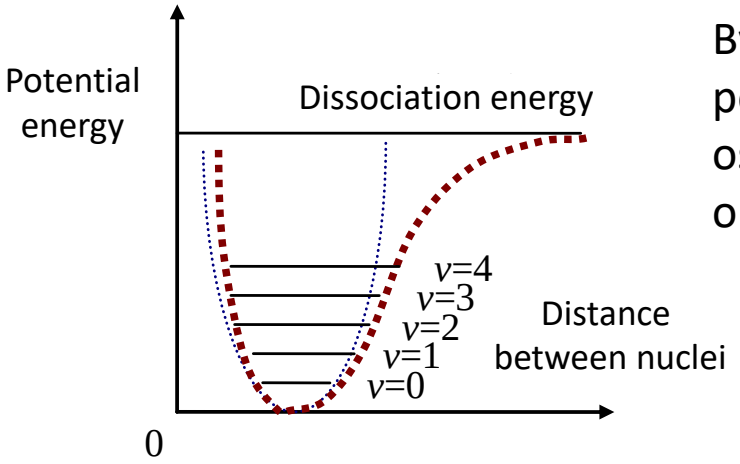

(b)

Non-harmonic oscillator

By solving the Schrödinger equation according to the potential energy function of the non-harmonic oscillator, the potential energy of the system can be obtained:

$$E = \left(v + \frac{1}{2}\right)hcv' - \left(v + \frac{1}{2}\right)^2 xhcv' + \cdots$$

The horizontal lines in the figure are the energy levels corresponding to each vibration quantum number ***v***. When the amplitude of atomic vibration is small, the harmonic oscillator model can be used approximately; when the amplitude is large, the harmonic oscillator model cannot be used.

13.7 Infrared Spectrum

- Infrared Spectroscopy and Molecular Vibrations

Normal vibration keeps the center of mass of the molecule unchanged, and there is no overall rotation. Each atom makes a simple harmonic vibration near its equilibrium position, and its vibration frequency and phase are the same. Any complex vibration in a molecule can be regarded as a linear combination of normal vibrations.

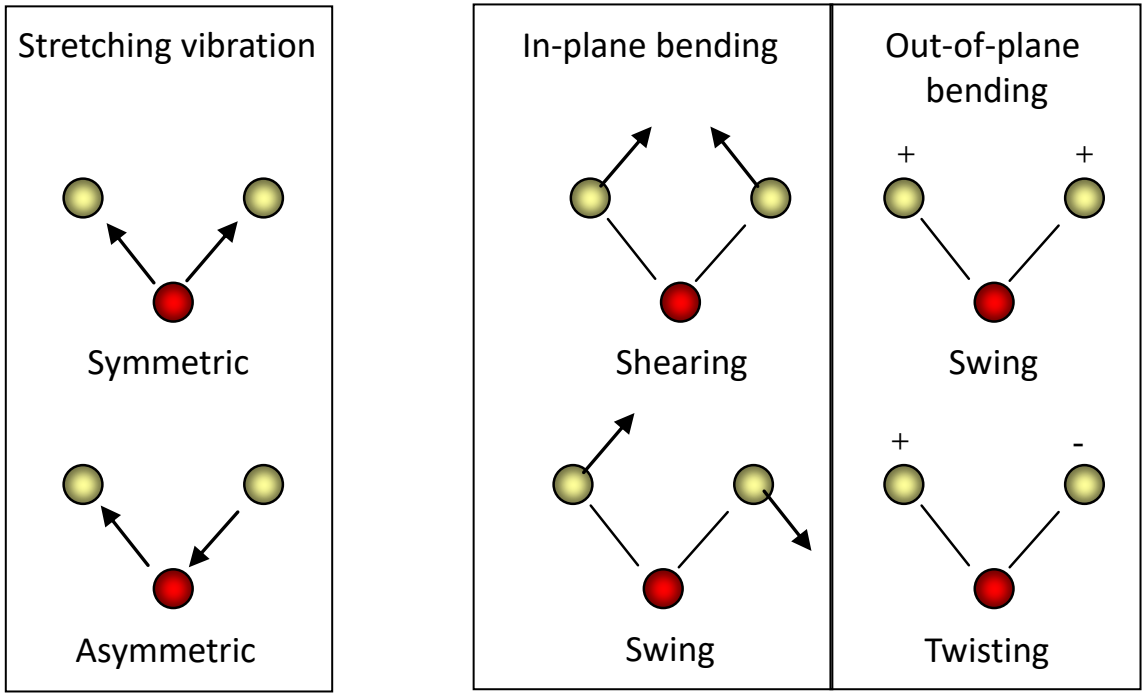

13.7 Infrared Spectrum

- Conditions for generating infrared spectrum

1) When the energy of infrared light is equal to the difference between the two energy levels of the molecule, the electromagnetic wave of this frequency will be absorbed by the molecule, causing a transition of the corresponding energy level of the molecule. The macroscopic manifestation is a decrease in the intensity of the transmitted light. This condition determines the location of the absorption peak. When an energy level transition occurs between two adjacent vibrational energy levels, it should satisfy:

$$\Delta E = E_{(v+1)} - E_{(v)} = hv$$

2) There is a coupling between infrared light and molecules. In order to meet this condition, the dipole moment of the molecules must change when they vibrate. This condition determines the intensity of the infrared band. The greater the change in dipole moment during vibration, the stronger the absorption band; the smaller the change in dipole moment during vibration, the weaker the absorption band.

13.7 Infrared Spectrum

- Conditions for generating infrared spectrum

Infrared spectra usually use wavelength or wave number as the abscissa to indicate the absorption peak position, and transmittance or absorbance as the ordinate to indicate the absorption intensity.

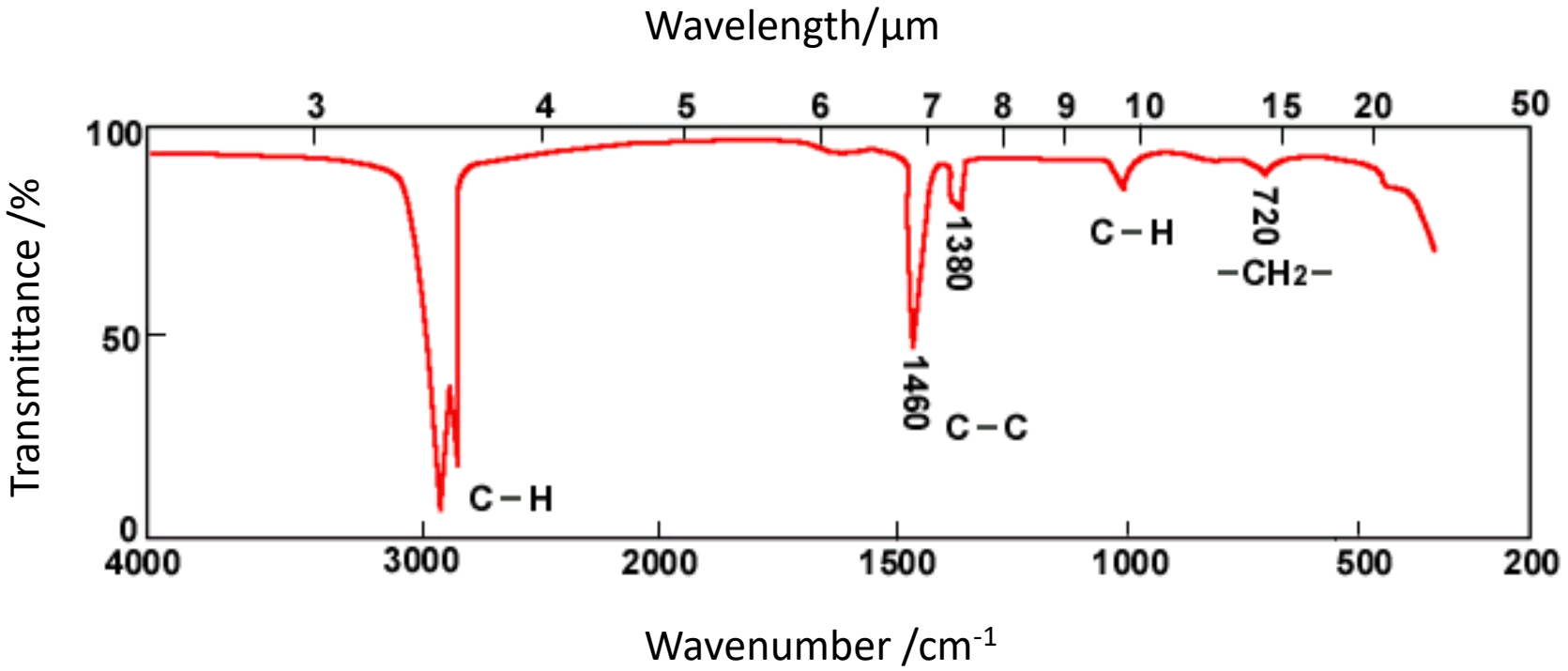

13.7 Infrared Spectrum

- Group vibration and infrared spectral region

According to the source of the absorption peak, the infrared spectrum with wave number 4000~400 cm^{-1} can be roughly divided into two regions.

- Group frequency area: wave number 4000 ~ 1300 cm^{-1}
- Fingerprint area: wave number is 1300 ~ 400 cm^{-1}

1. Group frequency area

Also called functional group area or characteristic area, the absorption peaks in the characteristic frequency area are generated by the stretching vibration of the group. Although the number is not large, it has obvious characteristics. Mainly used to identify functional groups.

2. Fingerprint area

The peaks in the fingerprint area are numerous and complex and have no obvious characteristics. However, when the molecular structure is slightly different, the absorption in this area will show subtle differences. Fingerprint areas are helpful in distinguishing structurally similar compounds.

13.7 Infrared Spectrum

- Factors affecting group frequency

1) Induction effect: Due to the different electronegativity of the substituent, the bond force constant is changed, causing the frequency of the group to shift.
2) Conjugation effect: The conjugation effect of atoms containing lone pairs of electrons shifts the absorption frequency to low wave numbers. For the same group, if the induction effect and the conjugation effect exist at the same time, when the induction effect is greater than the conjugation effect, the vibration frequency moves to a high wave number, and conversely, the vibration frequency moves to a low wave number.
3) Hydrogen bonding effect: The existence of hydrogen bonds reduces the stretching vibration frequency.
4) Vibrational coupling: When two groups with the same or similar vibration frequency are adjacent and have a common atom, the vibration frequency changes, one moves to high frequency, the other moves to low frequency, and the spectrum band splits.

13.7 Infrared Spectrum

- Infrared Spectroscopy Analysis Application

Infrared spectroscopic analysis is one of the important methods for material characterization. It is the most convenient and quick way to provide functional group information and can help determine some or even all molecular types and structures.

Qualitative analysis by infrared spectroscopy has the advantages of high characteristics, short analysis time, small amount of sample, no need to destroy the sample, and convenient measurement.

The quantitative analysis of infrared spectroscopy is based on Lambert-Beer's law. Its quantitative methods mainly include the direct calculation method, working curve method, absorption ratio method, and internal standard method, which are often used in the analysis of isomers.

Compared with other methods, infrared spectroscopy quantitative analysis still has some limitations, such as the requirement that the selected absorption peak must have sufficient intensity and not overlap with other peaks, so it can only be used under special circumstances.

13.8 Laser Raman Spectroscopy

- Overview and principles of Raman spectroscopy

The frequency of light that passes through a transparent medium and is scattered by molecules changes. Raman first discovered this phenomenon, so it is called Raman scattering, as shown in the figure.

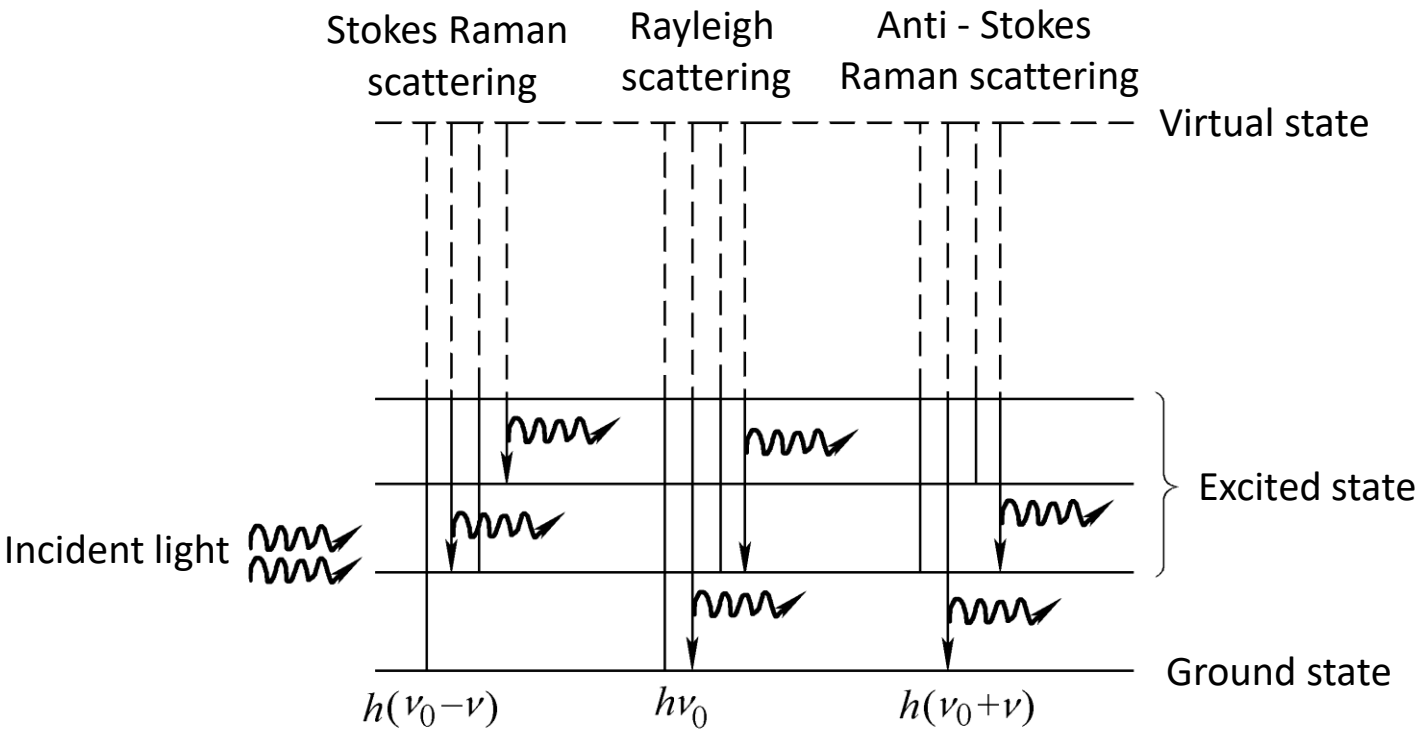

13.8 Laser Raman Spectroscopy

- Overview and principles of Raman spectroscopy

Assume that the incident photon energy is $h\nu_0$ and inelastic scattering occurs with the molecule. The molecule absorbs the photon with frequency ν_0. If the molecule emits $(\nu_0-\nu)$ photon and transitions to a high energy state, it is called Stokes scattering; if the molecule emits $(\nu_0+\nu)$ photon, it is called Stokes scattering. The photon transitions to a low energy state, which is called anti-Stokes scattering; if the molecule emits ν_0 photon, it is called Rayleigh scattering.

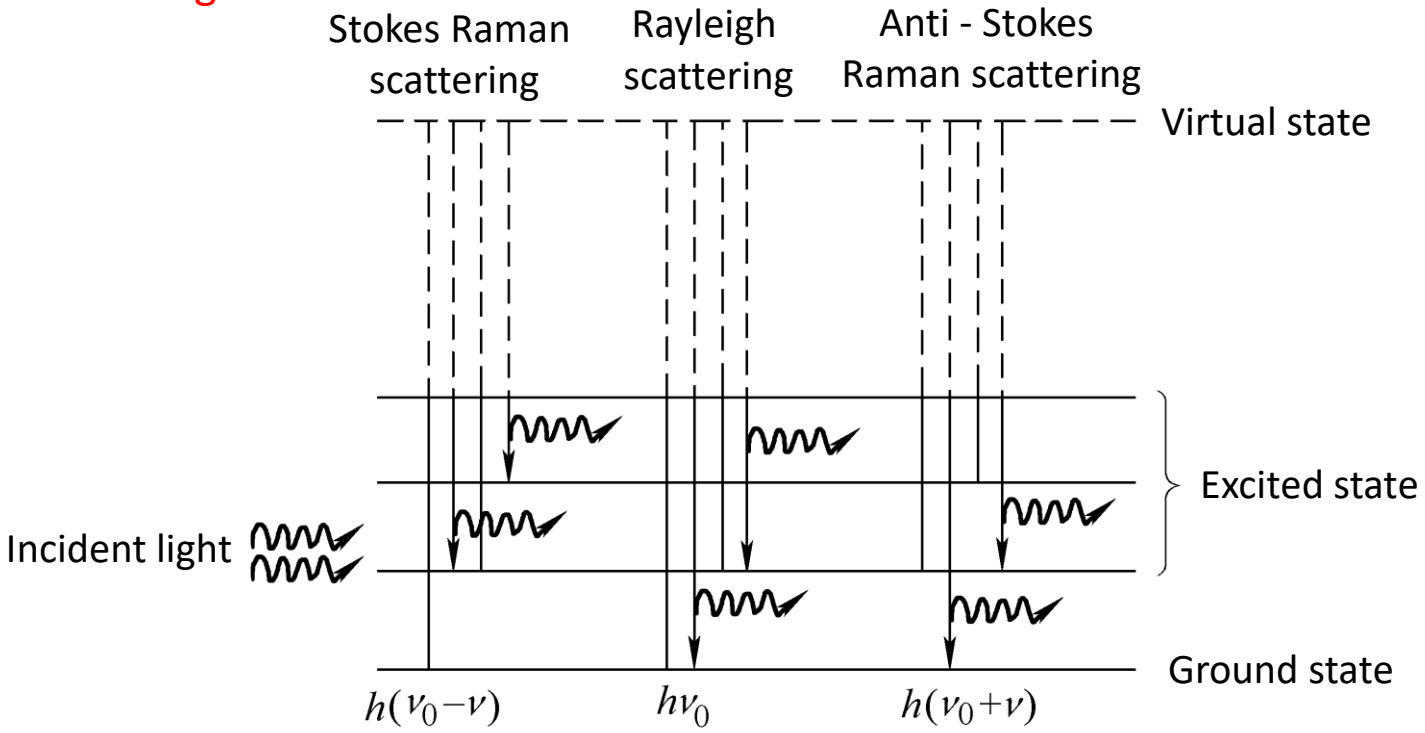

13.8 Laser Raman Spectroscopy

- Overview and principles of Raman spectroscopy

The spectral lines or bands $(\nu_0 \pm \nu)$ with frequencies symmetrically distributed on both sides of ν_0 are called Raman spectra. Among them, the component with smaller frequency $(\nu_0 - \nu)$ is called Stokes line, the component with larger frequency $(\nu_0 + \nu)$ is called anti-Stokes line, and the component with frequency ν_0 is called Rayleigh line.

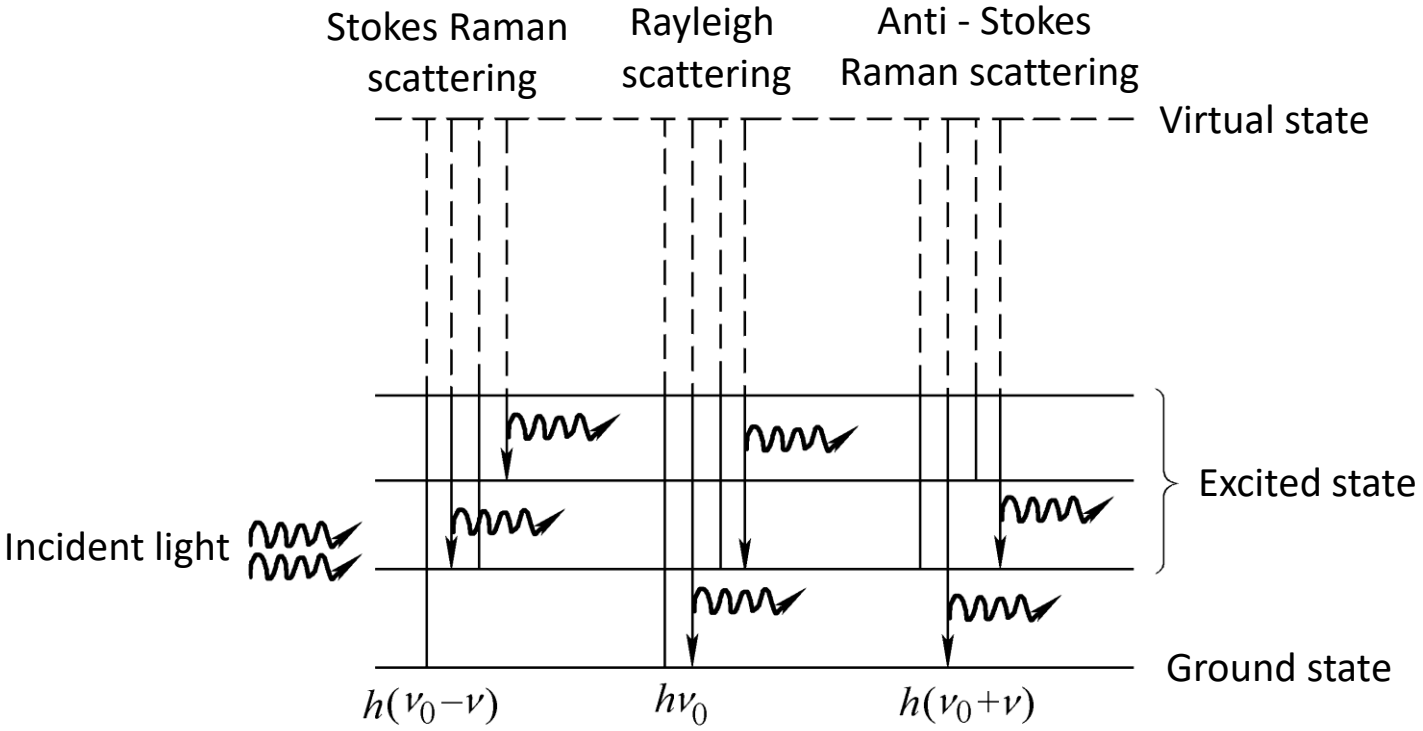

13.8 Laser Raman Spectroscopy

- Overview and principles of Raman spectroscopy

The spectral lines close to both sides of the Rayleigh scattering line are called small Raman spectrum; the spectral lines appearing on both sides far away from the Rayleigh line are called large Raman spectrum.

The small Raman spectrum is related to the rotational energy level of the molecule, and the large Raman spectrum is related to the vibration-rotational energy level of the molecule.

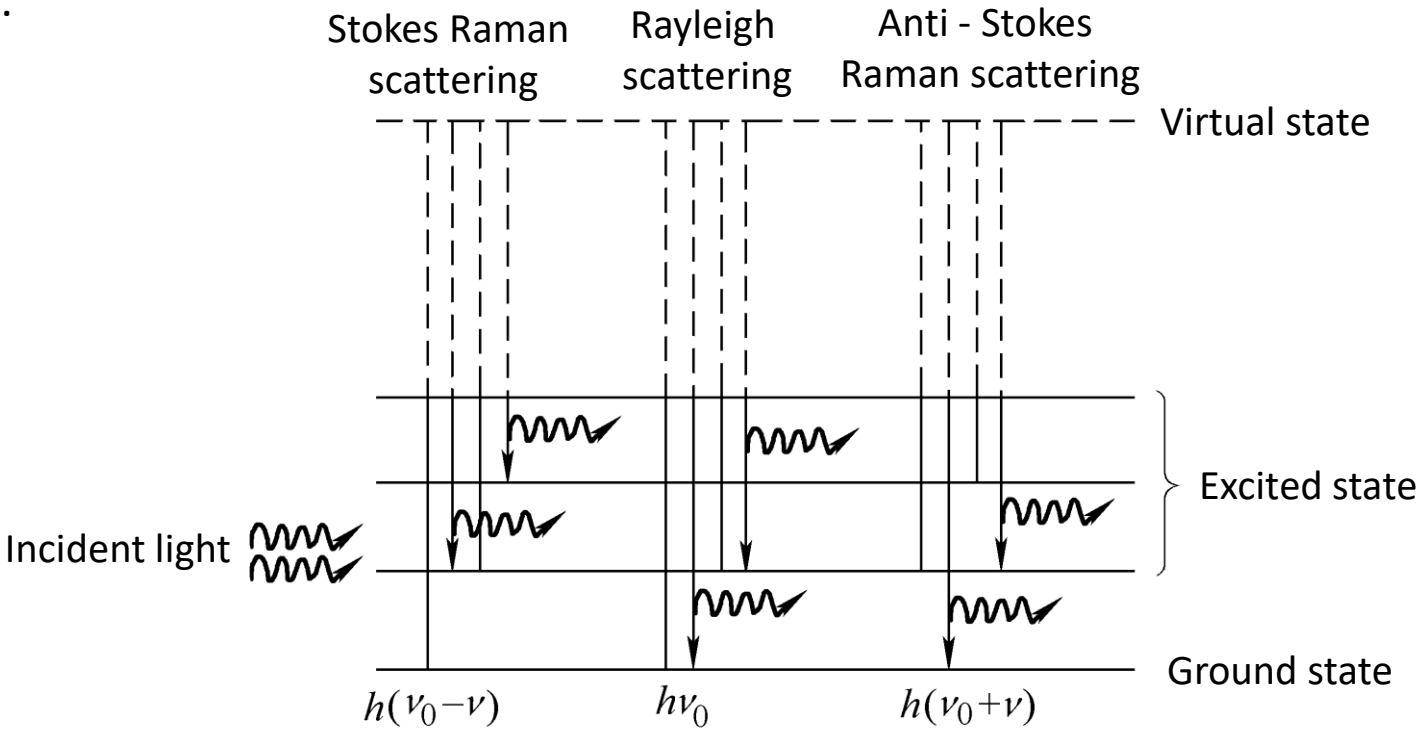

13.8 Laser Raman Spectroscopy

- Working principle of laser Raman spectrometer

The structure of a Raman spectrometer mainly includes a light source, external light path, dispersion system, receiving system, information processing and display, etc., as shown in the figure.

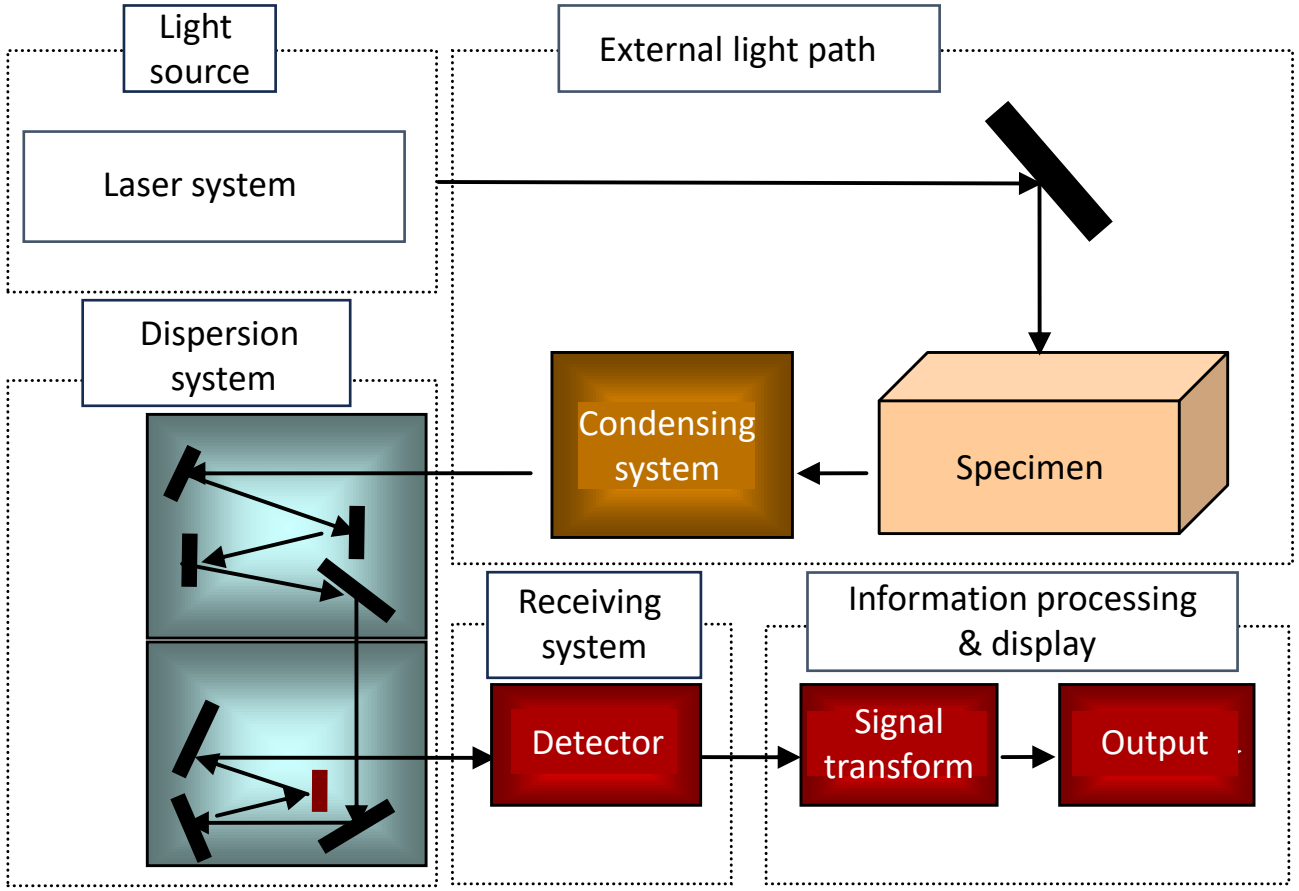

13.8 Laser Raman Spectroscopy

- Working principle of laser Raman spectrometer

1) Light source Currently, laser light sources with good monochromaticity, high intensity and stability are used.
2) External light path includes components such as light collection, light collection, sample holder, filter and polarization.
3) Dispersion system A monochromator is usually used to separate the Raman scattered light in space according to wavelength. Since the Raman scattering intensity is very weak, the Raman spectrometer is required to have a good level of stray light.
4) Receiving system: There are two types of reception of Raman scattering signals: single channel and multi-channel reception. Photomultiplier tube reception is single-channel reception.
5) Information processing and display: Common electronic processing methods used are DC amplification, frequency selection, and photon counting to extract Raman scattering information, and then a recorder or computer interface software is used to draw a map.

13.8 Laser Raman Spectroscopy

- Characteristics of Raman Spectroscopy

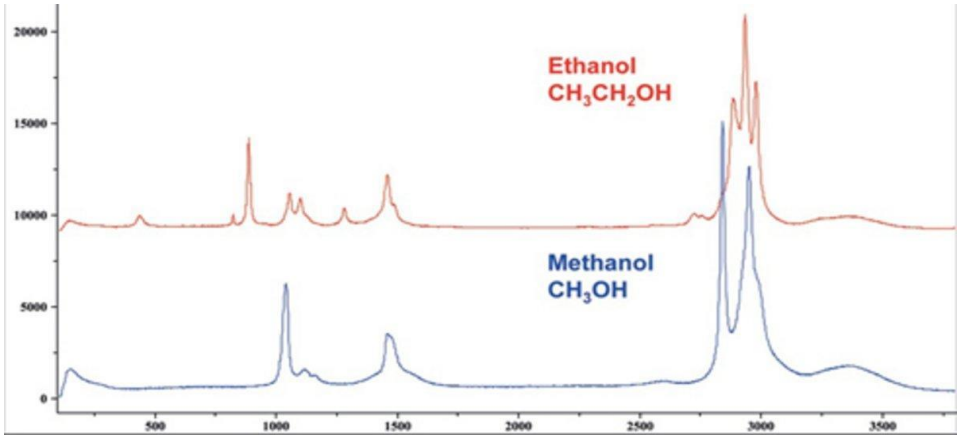

1) For the same sample, the displacement of the same Raman spectrum line has nothing to do with the wavelength of the incident light but is only related to the vibration and rotational energy levels of the sample molecules.
2) In the Raman spectrum with wave number as the variable, the Stokes lines and anti-Stokes lines are symmetrically distributed on both sides of the Rayleigh scattering line
3) Generally, the Stokes line is stronger than the Anti-Stokes line. This is because the number of particles in the vibrational ground state is much greater than in the vibrational excited state.
4) Raman spectroscopy can be used to determine the natural frequency of lattice vibration quickly.
5) The intensity of Rayleigh scattering rays only accounts for 10^{-3} of the intensity of incident light, and the intensity of Raman scattering is about 10^{-3} of Rayleigh scattering. That is, the intensity of Raman scattering is very weak.

13.8 Laser Raman Spectroscopy

- Comparison between infrared spectroscopy and Raman spectroscopy

Similarity:
For a given chemical bond, the infrared absorption frequency is equal to the Raman shift and can represent the energy of the first vibrational level. Both carry structural information that reflects the molecule.

Differences:
The wavelength of the incident light in the infrared spectrum is continuous, while the incident light in the Raman spectrum is monochromatic; the infrared spectrum detects the absorption of light, while the Raman spectrum detects the scattering of light. The generation mechanisms of the two are different.

The infrared spectrum mainly reflects the functional groups of the molecule, while the Raman spectrum mainly reflects the skeleton of the molecule; for molecules with a symmetry center, the two have a mutually exclusive rule: vibrations that are symmetrical to the symmetry center are invisible in the infrared, and Raman Visible; vibrations that have no symmetrical relationship with the symmetry center are visible in infrared and invisible in Raman

13.8 Laser Raman Spectroscopy

- Raman spectroscopy analysis applications

1) Qualitative and quantitative analysis Raman shift is the basis for qualitative molecular structure analysis and can be used in organic chemistry, polymers, biology, surfaces and films, etc.
2) Organic Chemistry Use the size, intensity and Raman peak shape of the Raman shift to identify the chemical bonds and functional groups of the molecule; use its polarization characteristics to determine the cis-trans structure.
3) High polymer Raman spectrum can provide structural information about carbon chains or rings. Used to determine isomers (mono-isomerism, positional isomerism, geometric isomerism, etc.)
4) Biology Since the Raman spectrum of water is very weak and the spectrum is very simple, Raman spectrum can study the structure and changes of biological macromolecules in a state close to the natural and active state.

13.9 UV-visible absorption spectrum

- Overview of UV-Visible Spectroscopy

1) The wavelength range of ultraviolet light is 10~400 nm, which is between visible light and X-rays. UV can be divided into A rays, B rays and C rays (i.e. UVA, UVB and UVC), with wavelength ranges of 315~400 nm, 280~315 nm, and 190~280 nm respectively.
2) UV-visible absorption spectroscopy, based on the absorption spectrum generated by intramolecular electronic transitions. This molecular absorption spectrum arises from transitions between electron energy levels of valence electrons and electrons in molecular orbitals. The absorption of molecules in the UV-visible region is closely related to their electronic structure, and most of the analysis objects are molecules with conjugated double-bond structures.
3) UV-visible absorption spectroscopy is widely used in the qualitative and quantitative analysis of organic and inorganic substances. The absorption wavelength range is 10~800 nm.
4) UV-visible absorption spectrometry has the advantages of high sensitivity, good accuracy, fast analysis speed, excellent selectivity and easy operation.

13.9 UV-visible absorption spectrum

- UV-visible spectrum generation mechanism

1. Molecular orbitals

The electrons in the molecule no longer belong to a certain atom, but move throughout the entire molecule space. Its motion state can be described by molecular orbitals ψ, and the orbital names are represented by symbols such as σ, π, δ...

Several atomic orbitals can be combined into several molecular orbitals. Half of the molecular orbitals are formed by the superposition of two atomic orbitals with the same sign, which are called bonding molecular (axially symmetric) orbitals, such as σ, π orbitals; the other half of the molecular orbitals are composed of the superposition of two atomic orbitals with opposite signs is called antibonding molecular (crystal plane symmetry) orbitals, such as σ^*, π^* orbitals.

Suppose there is no obvious difference between the energy of the molecular orbital after combination and the energy of the atomic orbital before combination. In that case, there are unbonded lone pairs of electrons in the molecule, called non-bonding electrons (***n*** electrons).

13.9 UV-visible absorption spectrum

- UV-visible spectrum generation mechanism

2. The principle of the linear combination of atomic orbitals

1) Principle of symmetry matching: Only atomic orbitals with matching symmetry can be combined.
2) Principle of energy approximation: Only atomic orbitals with similar energies can be combined.
3) The principle of maximum orbital overlap: the greater the degree of overlap, the lower the energy of the combined molecular orbitals.
4) The arrangement of electrons in molecular orbitals follows the same principle as the arrangement in atomic orbitals.
5) Bond level: The higher the bond level, the more stable the bond; the smaller the bond level, the longer the bond length.
6) Bond energy: At absolute zero, when the ground state molecule AB is disassembled into the ground state A and B atoms, the energy required is called the bond dissociation energy of the molecule, represented by the symbol D(A-B).
7) Bond angle: The angle between keys. If the bond lengths and bond angles are known, the geometric configuration of the molecule can be determined.

13.9 UV-visible absorption spectrum

- UV-visible spectrum generation mechanism

3. Electronic transition type

As shown in the figure, the relationship between molecular orbital energy is, $\sigma < \pi < n < \pi^* < \sigma^*$. When electrons absorb energy under the action of ultraviolet-visible light, six types of electronic transitions may occur: $n \rightarrow \pi^*$, $\pi \rightarrow \pi^*$, $n \rightarrow \sigma^*$, $\pi \rightarrow \sigma^*$, $\sigma \rightarrow \pi^*$, $\sigma \rightarrow \sigma^*$.

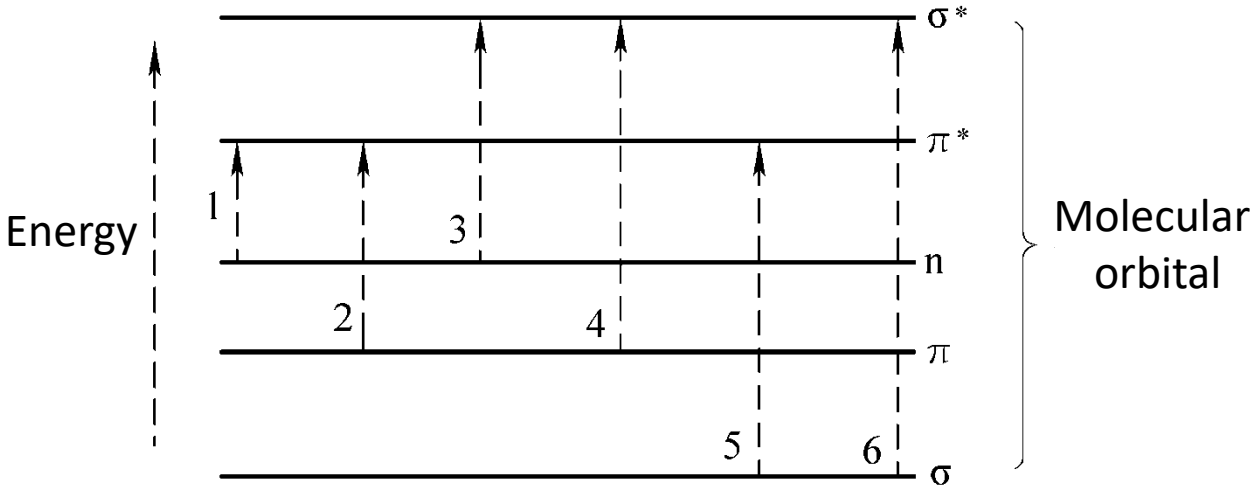

The type of electronic transition is closely related to the structure of the molecule and its groups, so the possible types of electronic transitions can be predicted based on the molecular structure.

13.9 UV-visible absorption spectrum

- Lambert-Beer law

As shown in the figure, a beam of parallel monochromatic light irradiates a colored solution. Suppose the incident light intensity is $\boldsymbol{I_0}$, the solution concentration is ***c***, the liquid layer thickness is ***b***, and the transmitted light intensity is $\boldsymbol{I}$, then,

$$\lg \frac{I_0}{I} = Kcb$$

In the formula, $\boldsymbol{\lg(I_0/I)}$ represents the degree to which light is absorbed through the solution, generally called absorbance (***A***) or extinction (***E***). Therefore, the above formula can be written as:

$$\boldsymbol{A = Kcb}$$

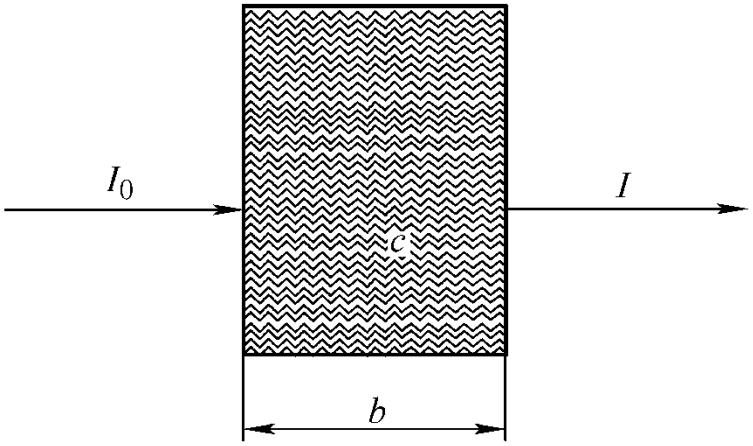

The formula is Lambert-Beer's law. It shows that the absorbance of the solution is proportional to the product of the solution concentration and the thickness of the liquid layer. In the formula, ***K*** is the absorption coefficient. For the same substance and a given incident light wavelength, ***K*** is a constant.

13.9 UV-visible absorption spectrum

- Characteristics of UV-visible absorption spectroscopy and its influencing factors

UV-visible absorption spectrum can reflect the energy level transition of valence electrons in molecules and is often used for quantitative analysis of conjugated systems. It has the advantages of high sensitivity and low detection limit. Factors affecting the UV-visible absorption spectrum include the conjugation effect, Hyperconjugation effect, solvent effect, and solvent pH value.

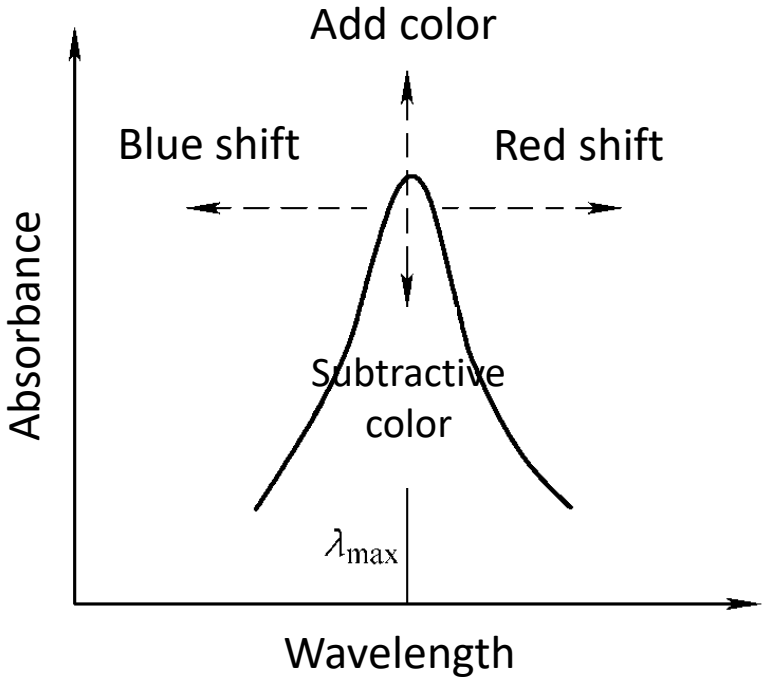

The impact of these factors on the absorption band results in band displacement (blue shift or red shift), band intensity change (increased or subtracted color), the appearance or disappearance of the fine structure of the band, etc., as shown in the figure.

13.9 UV-visible absorption spectrum

- Working principle of UV-visible absorption spectrometer

The UV-visible absorption spectrometer consists of a light source, a monochromator, an absorption cell, a detector, and a data processing and recording part. The working principle is shown in the figure.

Use separate dual light sources of deuterium lamp (185~395 nm) and tungsten lamp (350~800 nm), and a monochromator composed of a dispersion prism or diffraction grating to obtain multi-component monochromatic light of different wavelengths and send it through a slit, sample cell, and then enter the detector for detection.

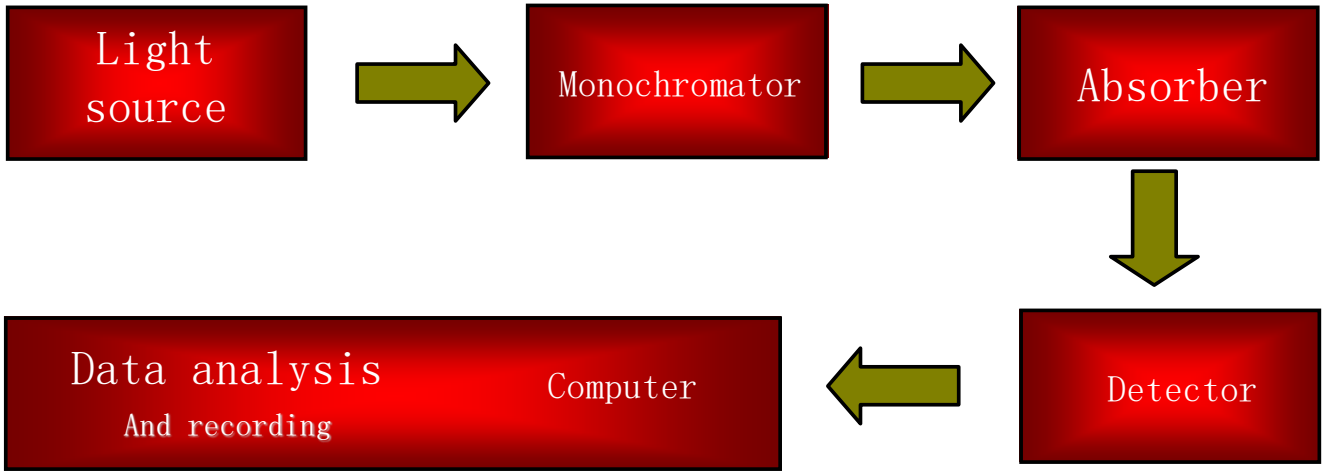

13.9 UV-visible absorption spectrum

- UV-visible spectroscopy applications

The ultraviolet absorption spectrum is the characteristic of the chromophore and auxochromophore in the molecule, not the characteristic of the entire molecule. Chromophore refers to an unsaturated group in a molecule that can absorb light radiation and has a transition, also called a chromophore.

1) Identification of compounds Identification of the conjugated structural system in the molecular skeleton.
2) Purity check: Use UV spectroscopy to check the purity of compounds.
3) Determination of isomers: Calculate the λ_{max} value and compare it with the measured value to determine the isomer type of the compound.
4) Determination of steric hindrance: Steric hindrance will affect the conjugated plane properties of the conjugated system.
5) Quantitative analysis: measure absorbance and perform quantitative analysis using Lambert-Beer's law.
6) Determination of hydrogen bond strength.

13.10 Atomic emission spectrum

- Overview of Atomic Emission Spectroscopy

The atoms or ions of each element have their own characteristic emission spectrum, so the sample can be qualitatively analyzed according to the wavelength of the characteristic spectral line; the element can be quantitatively measured according to the intensity of the characteristic spectral line, that is, atomic emission spectrometry. The method consists of three main processes:

1) The light source provides energy to evaporate the sample to form gaseous atoms, and further excites the gaseous atoms to produce optical radiation.

2) The composite light emitted by the light source is decomposed by a monochromator, and the spectral lines are arranged in wavelength order to form a spectrum.

3) Use a detector to detect the wavelength and intensity of the spectral lines in the spectrum.

13.10 Atomic emission spectrum

- Basic principles of atomic emission spectroscopy

After the ground state atoms absorb energy, they are in an excited state, and then transition to a low energy state or ground state, excess energy and emitting photons with characteristic frequencies, forming a series of characteristic spectral lines. The photon energy is the energy difference between the two energy levels ΔE.

$$\Delta E = \frac{hc}{\lambda}$$

In the formula, ***h*** is Planck's constant; ***c*** is the speed of light; λ is the characteristic wavelength of the emission spectral line. When atoms are excited, they may be in different excited states, and then may transition to different low energy levels or ground states in different forms, so they can emit different wavelengths, forming spectral lines. The characteristic spectral line intensity is ***I***.

$$I = N_i A h v$$

In the formula, N_i is the number of atoms in the i-th energy level per unit volume, ***A*** is the transition probability of electrons between a certain two energy levels, ***h*** is Planck's constant, and ***v*** is the spectral line frequency.

13.10 Atomic emission spectrum

- Atomic emission spectrometer composition

As shown in the figure, the atomic emission spectrometer mainly consists of three parts: an excitation light source, a spectroscopic system and a detector. In addition, it also includes signal processing and computer systems.

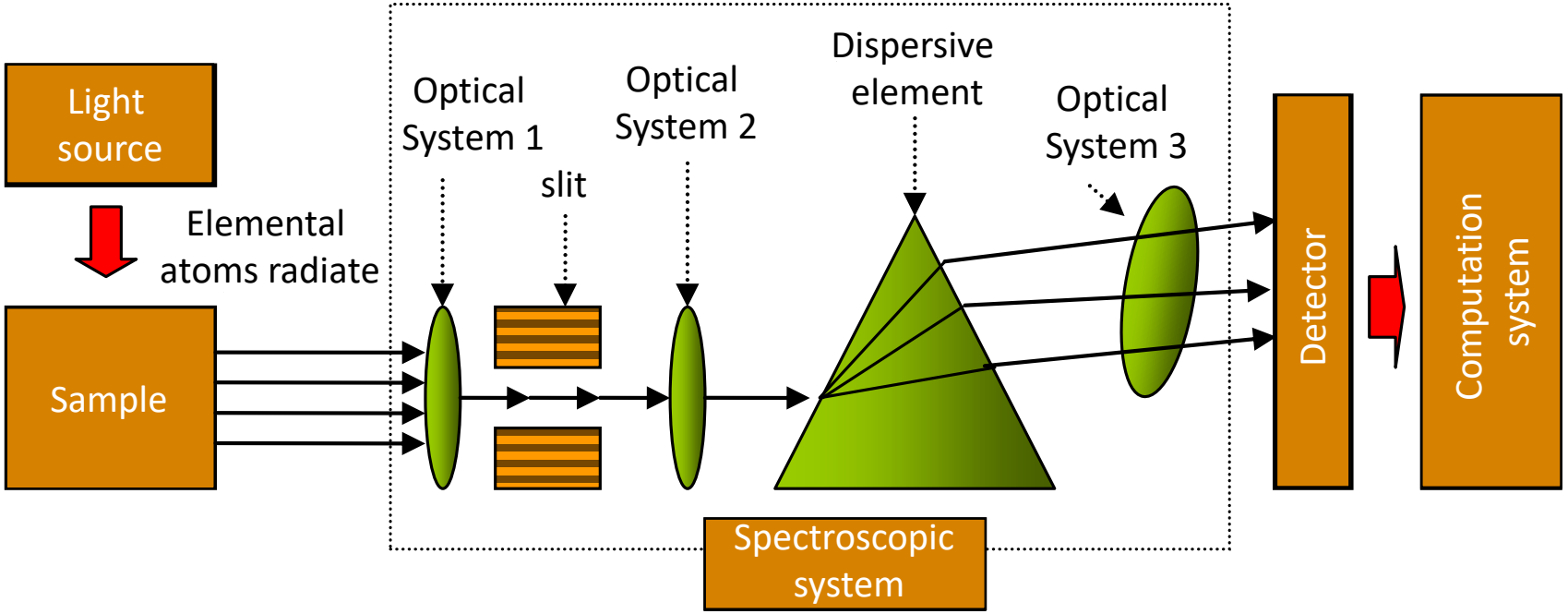

13.10 Atomic emission spectrum

- Atomic emission spectrometer composition

1) Excitation light source is used to evaporate, dissociate, atomize, excite, and transition the sample to produce optical radiation. Currently, commonly used light sources include flame, DC arc, AC arc, spark, laser, and inductively coupled high-frequency plasma (ICP). Among them, ICP light source has the advantages of high temperature, small matrix effect, low detection limit, and wide linear range. is an ideal light source.

2) The spectroscopic system is composed of some prisms and gratings. Its function is to disperse light of different wavelengths to form a spectrum.

3) Detector: The detection system should maintain stable performance and have good sensitivity, resolution, and spectral response range. Commonly used detection methods include the visual method, spectroscopy method, and photoelectric method. The solid-state imaging system has fast detection speed, large dynamic linear range, high sensitivity, and can detect multiple spectral lines simultaneously.

13.10 Atomic emission spectrum

- Applications and Characteristics of Atomic Emission Spectrometers

1. Characteristics of Atomic Emission Spectrometers

1) Simple operation, fast analysis, and no sample processing required.

2) High sensitivity: relative sensitivity 0.1~10 **μg/g**, absolute sensitivity 10^{-9} **g** or less.

3) Good selectivity. No chemical separation is required. Dozens of elements can be measured simultaneously under suitable conditions.

4) The amount of sample used is small, usually only a few milligrams to tens of milligrams.

5) Microanalysis has high accuracy. Usually, the relative error is only 5~20%. Especially when the content is <0.1%, the accuracy is better than that of chemical analysis.

6) It can only determine the elemental composition and content of a substance but cannot give information about the molecules and their structure of the substance.

13.10 Atomic emission spectrum

- Applications and Characteristics of Atomic Emission Spectrometers

2. Applications of Atomic Emission Spectrometers

1) Qualitative analysis: The spectral line with greater intensity in the characteristic spectrum of an element is usually called the sensitive line of the element. Whether the sensitive line of an element can be detected is the basis for whether the element exists.

2) Semi-quantitative analysis: Spectrograph is currently the most important means of semi-quantitative spectra analysis. It can quickly give the approximate element content to be measured in the sample. Commonly used methods include the spectral line blackness comparison method and visualization method.

3) Quantitative analysis is usually performed using the internal standard method to eliminate or reduce errors caused by various factors. The internal standard method uses the intensity ratio of the analysis line and the comparison line to analyze the element content quantitatively.

13.11 Atomic absorption spectroscopy

- Overview of Atomic Absorption Spectroscopy

As a practical analysis method, atomic absorption spectroscopy began in 1955; in the mid-1960s, atomic absorption spectroscopy entered a period of rapid development.

In recent years, a microcomputer-controlled atomic absorption spectrophotometer has been designed using a continuous light source and an echelle grating, combined with a photoconductive camera tube and a diode array multi-element analysis detector. It opens up new prospects for solving the problem of simultaneous determination of multiple elements.

Atomic absorption spectrometry determines the content of an element in the vapor phase based on the absorption intensity of the element's ground state atoms for its atomic resonance radiation.

This method is widely used in geology, metallurgy, machinery, chemical industry, agriculture, food, light industry, biomedicine, environmental protection, materials science and other research fields.

13.11 Atomic absorption spectroscopy

- Basic principles of atomic absorption spectroscopy

As shown in the figure, when radiation passes through the free atomic vapor, and the energy frequency required for the electrons in the atoms to enter a higher energy level is equal to the incident radiation, the atoms absorb energy, generating resonance absorption, and the electrons transition from the ground state to the excited state. This produces an atomic absorption spectrum.

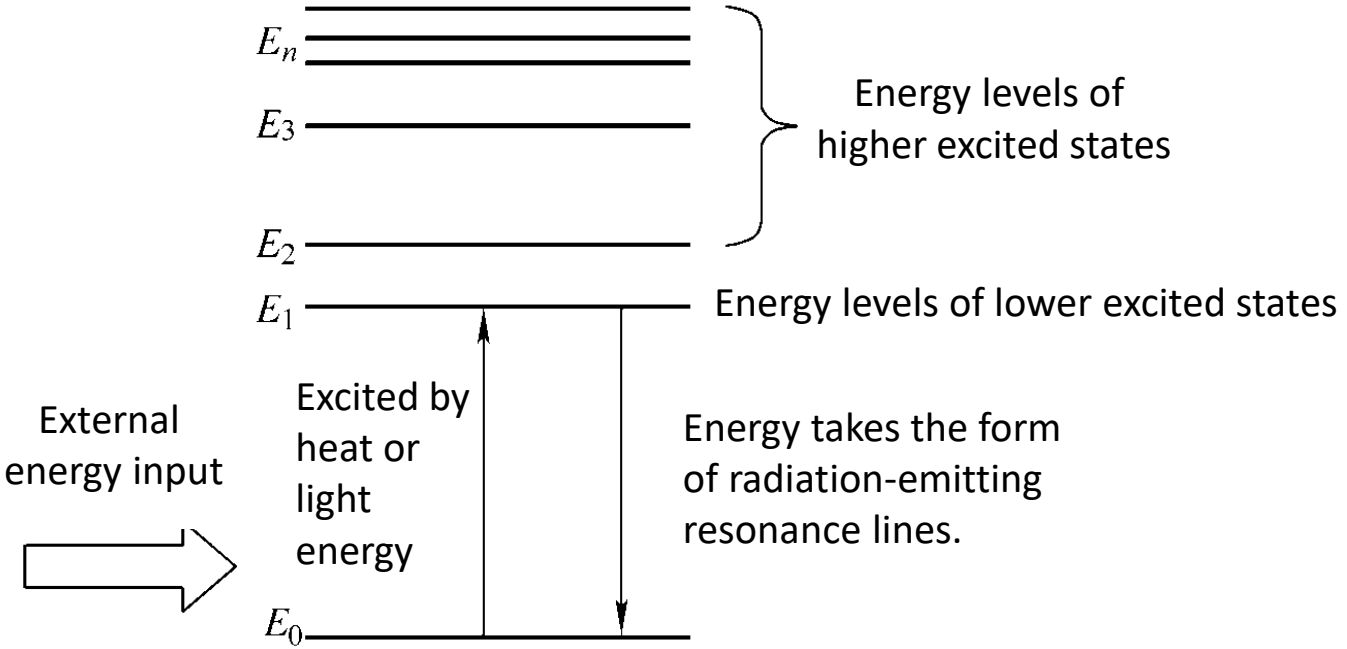

13.11 Atomic absorption spectroscopy

- Basic principles of atomic absorption spectroscopy

As shown in the figure, after a beam of incident light with intensity $\boldsymbol{I_0}$ passes through the atomic vapor, the transmitted light intensity is $\boldsymbol{I_x}$. Assuming the length of the atomic vapor is ***b***, the relationship between the incident light intensity and the transmitted light intensity is as follows:

$$I_{\mathrm{x}} = I_0 \, \mathrm{e}^{-K_{\mathrm{v}} b}$$

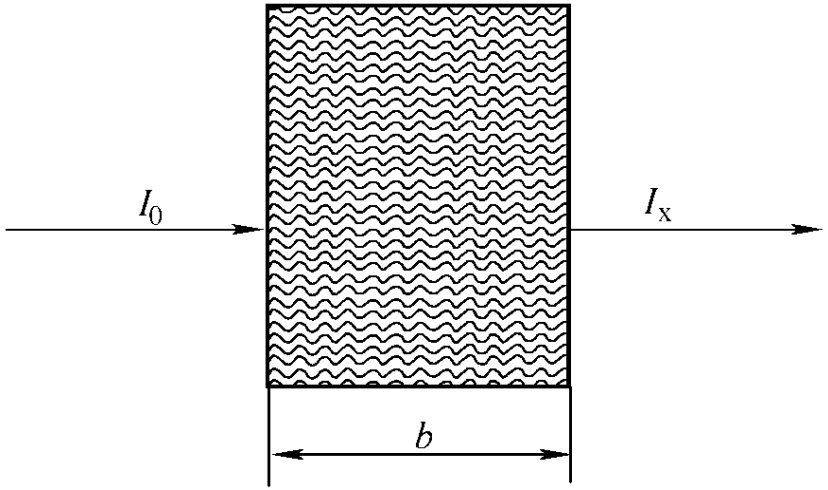

where, $\boldsymbol{K_v}$ is the atomic absorption coefficient. Because atoms selectively absorb radiation, the resonance absorption lines of each element have different characteristics. The energy absorbed when transitioning from the ground state to the first excited state is:

$$\Delta E = E_1 - E_0 = h\nu$$

13.11 Atomic absorption spectroscopy

- Basic principles of atomic absorption spectroscopy

Shown is the profile of an atomic absorption spectrum. Under certain conditions, the number of ground state atoms N_0 per unit volume of atomic vapor is proportional to the area of the absorption curve.

$$\int K_v dv = sN_0 = \frac{\pi e^2}{mc} fN_0$$

In the formula, ***e*** is the electron charge; m is the electron mass; ***c*** is the speed of light; N_0 is also called the ground state atomic density; ***f*** is the oscillator strength, which represents the average number of electrons absorbing characteristic light in each atom. Under certain conditions, for a certain element, ***f*** is a constant value.

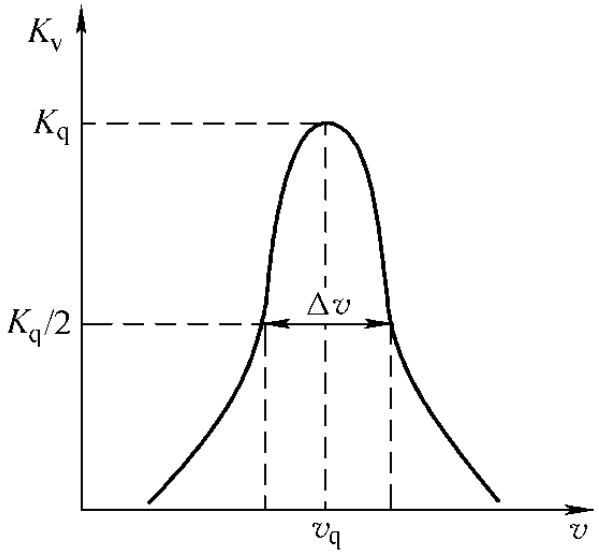

The above formula shows that the integral absorption is proportional to the number of ground state atoms that can absorb radiation per unit volume of atomic vapor. This is the theoretical basis for atomic absorption spectrometry analysis.

13.11 Atomic absorption spectroscopy

- Basic principles of atomic absorption spectroscopy

The profile of the absorption spectrum can be characterized by the center frequency of the spectral line and the half-maximum width Δv. The absorption peak K_q corresponding to the center frequency is:

$$K_q = \frac{2w}{\Delta v}\int K_v dv = \frac{2ws}{\Delta v} N_0$$

In the formula, ***w*** is the relevant constant for spectral line broadening. According to the definition of absorbance:

$$A = \log(\frac{I_0}{I_x}) = \log e^{K_v b} = 0.434 K_v b$$

At the peak point, then we have: $K_q = K_v$

Then: $A = 0.434 K_q b = 0.434 \frac{2ws}{\Delta v} N_0 b$

Once the system is determined, the absorbance ***A*** and N_0 are proportional, thus quantitative analysis can be carried out.

13.11 Atomic absorption spectroscopy

- Atomic absorption spectrometer composition

As shown in the figure, the atomic absorption spectrometer consists of a light source (such as a hollow cathode lamp), an atomization system, a spectroscopic system (such as a monochromator) and a detection system.

1) Light source used to emit characteristic resonance radiation of the measured element.

2) The atomizer is the main component of the atomic absorption spectrometer. It uses the flame to turn the elements in the test solution into atomic vapor.

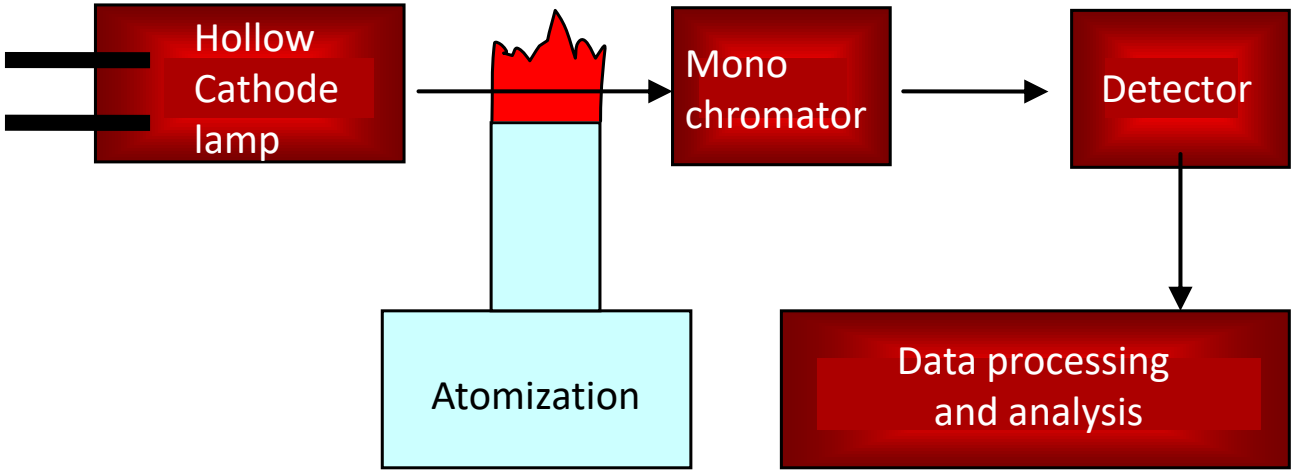

13.11 Atomic absorption spectroscopy

- Atomic absorption spectrometer composition

As shown in the figure, the atomic absorption spectrometer consists of a light source (such as a hollow cathode lamp), an atomization system, a spectroscopic system (such as a monochromator) and a detection system.

3) The spectroscopic system (monochromator) consists of a concave reflector, a slit or a dispersion element. The dispersion element is a prism or diffraction grating, which is used to separate the required resonance absorption lines.

4) The detection system comprises a detector, amplifier, logarithmic converter and computer. After amplifying and converting the signal, the computer system is used to process the output.

13.11 Atomic absorption spectroscopy

- Characteristics of Atomic Absorption Spectroscopy

1) Strong selectivity. Because the atomic absorption bandwidth is very narrow, the measurement is fast and simple, and there are conditions for automated operation.

2) High sensitivity. It is one of the most sensitive methods currently. Most elements in routine analysis can reach the ppm (1/1,000,000) level.

3) Wide analysis range. There are 73 elements that can be measured, and it is suitable for determining major elements, low elements, trace elements, and trace elements.

4) Strong anti-interference ability. Compared with the atomic emission spectrum, the influence of the third component and plasma temperature on the intensity of the atomic absorption spectrum line is relatively small.

5) High precision. The flame atomic absorption method has good precision. For the determination of low-amount elements, the precision is generally 1~3%.

13.12 Nuclear Magnetic Resonance (NMR)

- NMR Overview

In 1930, it was discovered that atomic nuclei in a magnetic field would be aligned in an orderly and parallel manner in the direction of the magnetic field, either forward or reverse. After applying radio waves, the spin direction of the nuclei flips.

In 1946, it was discovered that when an atomic nucleus with an odd number of nucleons (including protons and neutrons) is placed in a magnetic field, and a radio frequency field of a specific frequency is applied, the nucleus absorbs the energy of the radio frequency field.

After 1990, NMR has been widely used in molecular composition and structure analysis, biological tissue and living tissue analysis, pathological analysis, medical diagnosis, and non-destructive product monitoring. The emergence of pulsed Fourier transform NMR instruments has led to an increasing number of applications of 13C spectroscopy.

13.12 Nuclear Magnetic Resonance (NMR)

- Principles of NMR

The phenomenon of nuclear magnetic resonance originates from the movement of the spin angular momentum of the atomic nucleus under the action of an external magnetic field. According to the principles of quantum mechanics, like electrons, atomic nuclei have spin angular momentum, whose size is determined by the spin quantum number ***I*** of the nucleus.

If the mass number and the number of protons are both even, ***I*** = 0;

If the mass number is an odd number, ***I*** = ***n/2*** (***n***=1, 3, 5,...);

If the mass number is even and the number of protons is odd, ***I*** = ***n/2*** (***n***=2, 4, 6,...)

That is, different types of atomic nuclei have different spin quantum numbers. So far, only the nuclei with ***I*** = ***n/2*** (***n***=1, 3, 5,...), and their nuclear magnetic resonance signals are used. Generally used nuclei are: $^{1}\mathbf{H}$, $^{11}\mathbf{B}$, $^{13}\mathbf{C}$, $^{17}\mathbf{O}$, $^{19}\mathbf{F}$, $^{31}\mathbf{P}$

13.12 Nuclear Magnetic Resonance (NMR)

- Principles of NMR

When the atomic nucleus spins, it will spin to produce a magnetic moment whose component in the ***z*** direction is μ_z.

$$\mu_Z = \gamma P_Z = \gamma \frac{h}{2\pi} m$$

In the formula, γ is the magnetic spin ratio, and the larger γ is, the stronger the magnetism; ***m*** is the magnetic quantum number of the atomic nucleus.

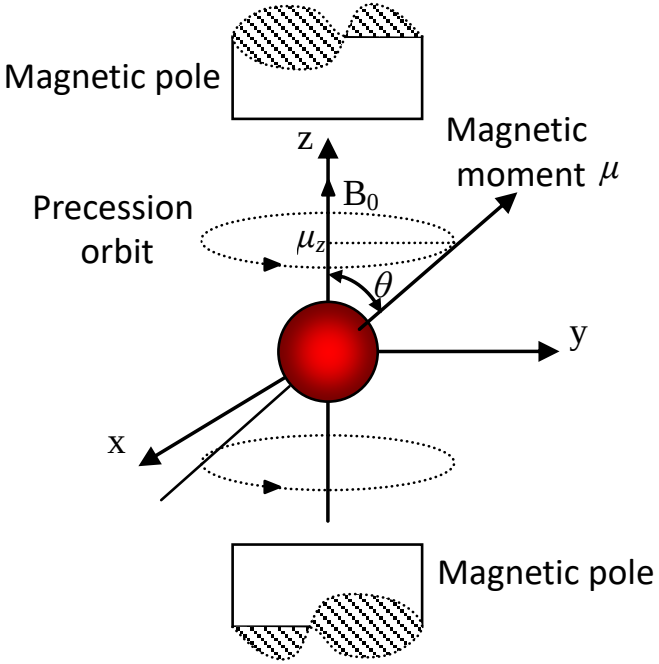

As shown in the figure, when the atomic nucleus is placed in an external magnetic field $\boldsymbol{B_0}$, the direction of the nuclear magnetic moment is different from that of the external magnetic field. The nuclear magnetic moment will rotate around the direction of the external magnetic field. This phenomenon is called precession, and the precession frequency is ***v***.

$$v = \frac{\gamma}{2\pi} B_0$$

The precession frequency is determined by $\boldsymbol{B_0}$ and the properties of the nucleus itself.

13.12 Nuclear Magnetic Resonance (NMR)

- Principles of NMR

Under an external magnetic field, the energy of the magnetic core is:

$$E = -\mu B_0 \cos\theta = -\gamma \frac{h}{2\pi} B_0 m$$

In the formula, θ is the angle between the nuclear magnetic moment μ and the external magnetic field B_0. The energy of precession of the atomic nucleus is related to the magnetic field, the magnetic moment of the atomic nucleus, and the angle between the magnetic moment and the magnetic field.

In an external magnetic field, when the atomic nucleus absorbs other energy, an energy level transition will occur. The energy change ΔE caused by the transition is:

$$\Delta E = \gamma \frac{h}{2\pi} B_0$$

If the energy provided by the external radio frequency field is $h\nu_0$, and $h\nu_0 = \Delta E$, it will cause the atomic nucleus to transition between two energy levels, forming a nuclear magnetic resonance, and its resonance frequency is:

$$\nu_0 = \frac{\gamma}{2\pi} B_0$$

13.12 Nuclear Magnetic Resonance (NMR)

- Relaxation process

Relaxation in NMR can be divided into two categories according to its mechanism:

One type is spin-lattice relaxation. After the radio frequency field is turned off, the spin core and the surrounding lattice transfer energy to each other, causing the particle state to exhibit a Boltzmann distribution, also known as longitudinal relaxation, also known as T_1 relaxation. This process is an energy exchange process between the system and the environment. As a result, the number of high-energy level nuclei is reduced and the energy of the entire spin system is reduced. The smaller T_1, the higher the efficiency of longitudinal relaxation, which is more conducive to the detection of NMR signals.

Another type of spin-spin relaxation. After the radio frequency field is turned off, due to the different chemical environments of each resonance nucleus, their phases gradually return to asynchronous, and the distribution of the entire resonance nucleus system meets the requirements of the Boltzmann equilibrium state. This process is a transverse relaxation process. Also called T_2 relaxation. This process is an energy exchange between two nuclei with the same spin frequency. Energy is not lost, but the orientation of the two nuclei is changed.

13.12 Nuclear Magnetic Resonance (NMR)

- Chemical shift

In a constant radio frequency field, the resonance frequency of the same type of nucleus is not a constant value, but changes with the chemical environment in which the nucleus is located.

In the previous discussion, the atomic nucleus was treated as an isolated particle, and the existence of electrons outside the nucleus was not considered. In fact, due to electrons outside the nucleus, a new induced magnetic field will be formed due to the induction of the external magnetic field $\boldsymbol{B_0}$, as shown in the figure. The direction of the induced magnetic field is opposite to $\boldsymbol{B_0}$, and the magnitude is proportional to $\boldsymbol{B_0}$.

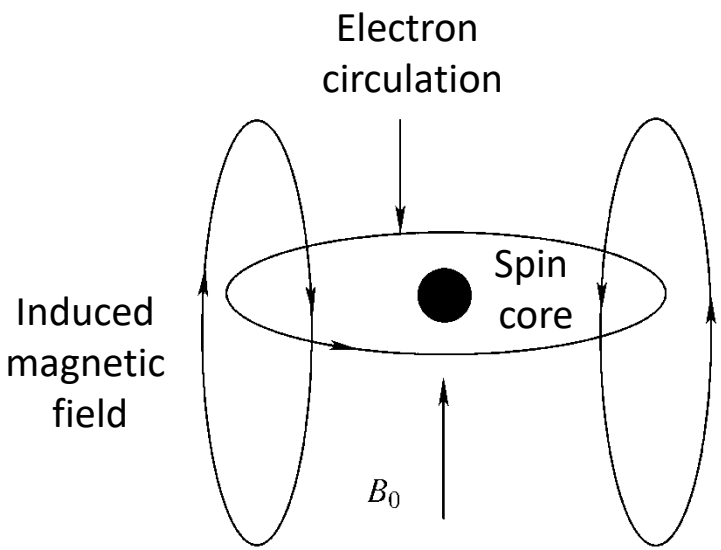

$$\boldsymbol{B_N = B_0(1-\sigma)}$$

In the formula, σ is the shielding constant, which describes the shielding effect of the extranuclear electron cloud on the nucleus.

13.12 Nuclear Magnetic Resonance (NMR)

- Chemical shift

Due to the existence of electron cloud outside the nucleus, the induced magnetic field formed has a shielding effect on the atomic nucleus, and the corresponding resonance frequency is corrected as:

$$\nu = \frac{\gamma}{2\pi} B_0 (1-\sigma)$$

Obviously, under different chemical environments, the resonance frequency of the same atomic nucleus changes in different ways. However, the frequency difference is very small, and it is difficult to determine its accurate value.

Use the standard material as the benchmark to measure the difference in resonance frequency between the sample and the standard material. Use δ to represent the chemical shift, and we have:

$$\delta = \frac{B_{St} - B_{sa}}{B_{St}} \times 10^6 = \frac{\nu_{St} - \nu_{sa}}{\nu_{St}} \times 10^6$$

In the formula, $B_{standard}$, B_{sample}, $\nu_{standard}$, and ν_{sample} are the external magnetic field intensity and magnetic nuclear resonance frequency of the standard material and the magnetic nuclei in the sample, respectively.

13.12 Nuclear Magnetic Resonance (NMR)

- Coupling constant

The phenomenon of spectral line splitting caused by mutual coupling using valence electrons as the medium between nuclei is called spin splitting. In the multiple peaks formed by spin splitting, the distance between two adjacent peaks is called the spin-spin coupling constant, represented by ${}^{n}J_{A\text{-}B}$.

As shown in the figure, for two spin nuclei A and B with opposite orientations, the spin orientations of the two adjacent valence electrons should be antiparallel. The change in the state of the two spin nuclei will be transferred to each other through the bonding electrons, resulting in energy level splitting.

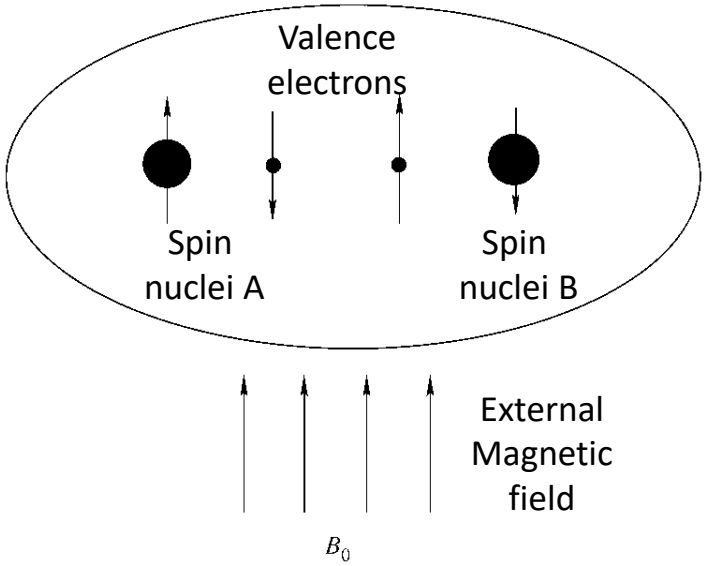

The main factors that affect the coupling constant are: atomic nuclear magnetism, such as nuclear gyromagnetic ratio; and molecular structure, such as bond length and bond angle; in addition, the electronegativity of the substituent, orbital hybridization, etc.

13.12 Nuclear Magnetic Resonance (NMR)

- NMR spectrometer

According to the radio frequency irradiation method, NMR spectrometers are divided into two categories, namely continuous spectrum NMR spectrometers and pulsed Fourier transform NMR spectrometers. The basic structure of a continuous spectrum NMR spectrometer is as shown in the figure. It mainly consists of a magnet, a radio frequency generator, a detector, a scanning unit, a signal processor and a computer system.

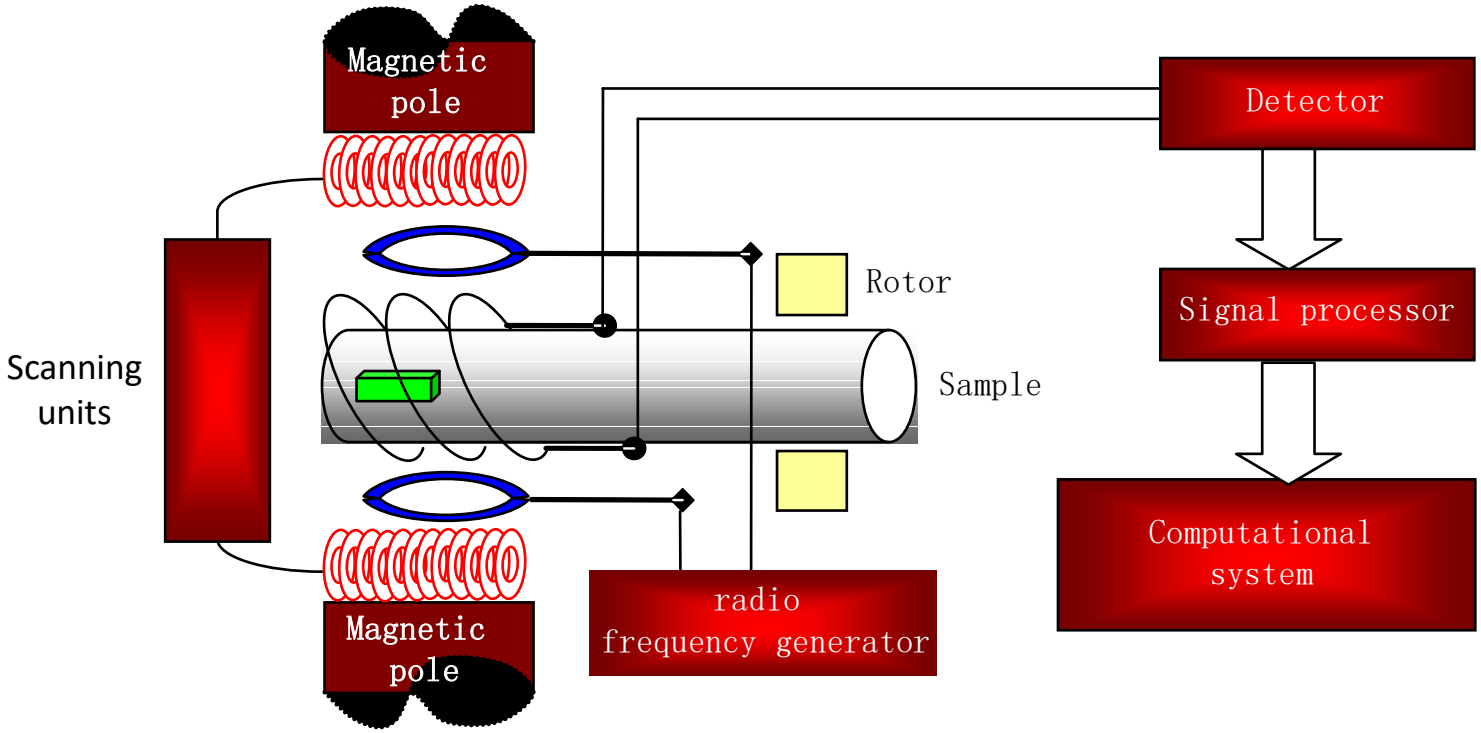

13.12 Nuclear Magnetic Resonance (NMR)

- NMR spectrometer

1) Qualitative analysis: NMR spectrum is an important tool for structural analysis. Chemical shifts can provide information on the nuclear environment. Peak multiplicity can provide information on adjacent groups and stereochemistry. Coupling constant values can be used to determine the substitution of groups. The peak intensity can determine the number of protons in the group, etc.

2) Quantitative analysis: Compared with other nuclei, $^{1}\mathbf{H}$ NMR spectrum is more suitable for quantitative analysis. The basic basis of quantitative analysis is that the area of a certain type of hydrogen nucleus resonance absorption peak is proportional to the number of corresponding hydrogen nuclei. The basic formula is:

$$A = nCA_0$$

In the formula, ***A*** is the peak area of a certain type of hydrogen nucleus in the compound to be tested; ***n*** is the number of a certain type of hydrogen nucleus in 1 mol of the compound to be tested; ***C*** is the number of moles of the compound to be tested; A_0 is the peak area of one hydrogen nucleus.

13.13 Electron energy loss spectrum

- Overview

- In the 1970s, the photoionization electron spectroscopy method was pioneered to study the energy level structure of molecules. Various electron spectrometers and collision methods were rapidly developed, including the electron energy loss spectroscopy (EELS) method.

- EELS is an effective electron microscopy analysis method that detects the characteristic energy lost by transmitted electrons when penetrating the sample to study the elemental composition, chemical bonding, and electronic structure of the material.

- The energy resolution of EELS is very high, better than 1 eV; it can detect a wide range of elements, namely $\mathbf{H^{1}}$~$\mathbf{U^{92}}$, and is more suitable for light elements; the high-energy loss area is mainly used for qualitative and quantitative analysis of elements, chemical valence state and density of state analysis, etc.

- Energy filtering imaging technology can eliminate the image background caused by inelastic scattering and improve image contrast; it can also be used to analyze the concentration distribution of elements.

13.13 Electron energy loss spectrum

- Principle of electron energy loss spectrum

Incident electrons interact with atoms in the film sample and undergo elastic and inelastic scattering. The energy loss of a part of the inelastically scattered electrons has a characteristic value, which is called characteristic energy loss electrons. Using an electrostatic or electromagnetic energy analyzer to disperse electrons according to their energy, the electron energy loss spectrum can be obtained.

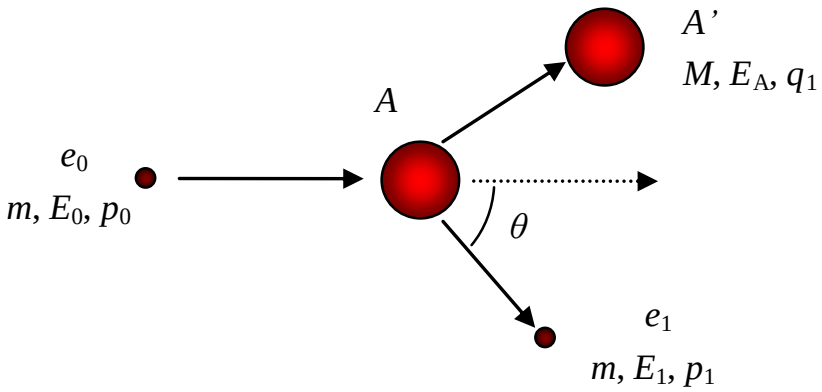

The picture shows a schematic diagram of scattering between electrons and atoms (molecules). e_0, e_1, A, and A' are the incident electrons, scattered electrons, target atoms, and energetic atoms, respectively. The masses of the electrons and atoms (molecules) are m and M, respectively. The incident electrons The kinetic energy and momentum of the scattered electrons are E_0, p_0, E_1, and p_1, respectively. The kinetic energy and momentum of the energized atom are E_A and q_1, respectively, θ is the scattering angle.

13.13 Electron energy loss spectrum

- Principle of electron energy loss spectrum

Inelastic collision causes the incident electron to lose part of its kinetic energy, and this energy is equal to the difference between the ground state energy before the collision (between the atom and the electron) and the excited state energy after the collision. The basic process of electron and atom scattering is as follows.

$$e_0(E_0, \vec{p}_0) + A \rightarrow e_1(E_1, \vec{p}_1) + A'(E_A)$$

According to the law of conservation of energy and momentum, the energy of the scattered electrons can be obtained as:

$$E_1 = \frac{1}{(m+M)^2}\left[(M^2 - m^2)E_0 - (m+M)ME_u + 2m^2\cos^2\theta E_0 \right.$$
$$\left. + 2m\cos\theta E_0\sqrt{m^2\cos^2\theta + (M^2 - m^2) - (m+M)ME_u / E_0}\right]$$

In the formula, E_u is the excitation energy of atoms (molecules). When inelastic scattering occurs, the energy loss E of the incident electron is approximately the excitation energy, that is:

$$E = E_0 - E_1 \approx E_u$$

13.13 Electron energy loss spectrum

- Basic structure and working principle of electron energy loss spectrometer

The electron energy loss spectrometer is mainly composed of an electron energy analyzer and an electronic detection system. After the electrons pass through the electron energy analyzer, they will be distributed according to the electron energy on the energy dispersion plane.

Early electron energy loss spectrometers used a serial electronic detection system, and its detection components could only process one energy channel at a time. To obtain the entire energy characteristic spectrum, each energy channel must be detected one by one, so the work efficiency was low.

Multiple quadrupole lenses are used to amplify and project the electron energy distribution onto a fluorescent screen, allowing one- or two-dimensional detection components composed of photodiodes or charge-coupled detectors to record multiple energy channels in parallel.

There are two types of electron energy loss spectrometers: magnetic prism spectrometers and filters. The former is installed under the transmission electron microscope photography system, and the latter is installed inside the lens barrel.

13.13 Electron energy loss spectrum

- Basic structure and working principle of electron energy loss spectrometer

As shown in the figure, the magnetic prism meter mainly consists of a sector magnet, a slit diaphragm and a signal receiving and processor. Transmitted electrons with different energies move along arc-shaped trajectories with different curvature radii under the influence of the magnetic field of the sector-shaped magnetic prism. Electrons with smaller energy have a smaller trajectory radius, while electrons with greater energy have a larger trajectory radius.

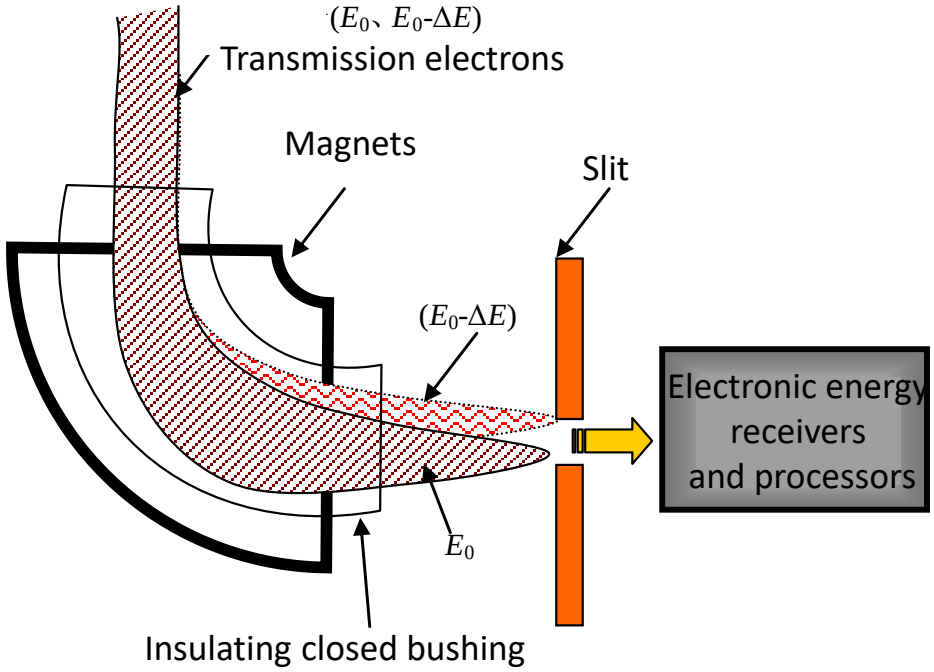

The electron energy and intensity are detected and calculated using the displacement difference between energy-loss electrons and zero-loss electrons on the focusing plane.

13.13 Electron energy loss spectrum

- Characteristics of electron energy loss spectrum and its applications

The figure is the electron energy loss spectrum of BN compounds. EELS can be divided into three regions, zero loss region, low energy loss region (5 ~50 eV) and high energy loss spectral region (>50 eV). The zero-loss region includes the contribution of unscattered and fully elastically scattered transmitted electrons, as well as partial quasi-elastically scattered transmitted electrons with energies less than 1 eV.

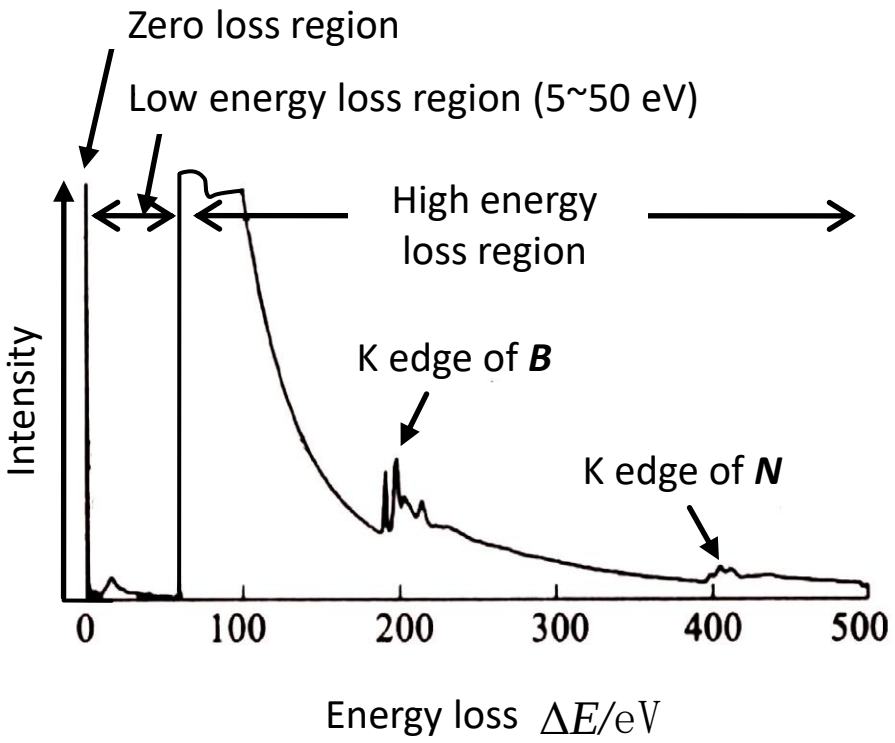

The intensity of the zero-loss peak is very high and is generally used for peak position correction, energy resolution determination, and zero-loss electron filter imaging to eliminate the electron diffraction pattern background and improve image contrast.

13.13 Electron energy loss spectrum

- Characteristics of electron energy loss spectrum and its applications

The low-energy loss region is composed of a plasma peak and several inter-band transition small peaks produced by the inelastic scattering of incident electrons and valence electrons of atoms in the solid. The energy loss of incident electrons caused by plasma excitation is:

$$\Delta E_{\mathrm{p}} = h\omega_{\mathrm{p}}$$

In the formula, ***h*** is Planck's constant; $\boldsymbol{\omega_p}$ is the plasma oscillation frequency. The plasma oscillation frequency is a function of the number of free electrons participating in the oscillation.

The ratio of the first intensity caused by plasma oscillation to the zero-loss peak intensity is related to the ratio of the sample thickness to the plasma oscillation mean free path, while the plasma oscillation mean free path is related to the incident electron energy and sample composition.

The low-energy loss zone can obtain information about sample thickness, micro-area chemical composition, electron density, electronic structure and dielectric constant.

13.13 Electron energy loss spectrum

- Characteristics of electron energy loss spectrum and its applications

The high-energy loss region has a rapidly attenuating background and an absorbing edge. The excitement of inner shell electrons such as K, L, and M of the element generates the ionization absorption edge. The starting energy of the ionization loss peak is the minimum energy required for the ionization of inner shell electrons, which can be used as the only characteristic energy for element identification—qualitative and quantitative analysis of elements.

Near the ionization loss peak threshold, the shape of the loss spectrum is a function of the electron density of atomic vacancy bound states in the sample. The electrons of excited atoms can enter the bound state and become a spectrum-shaped energy-loss near-edge structure. In the range of hundreds of electron volts from the ionization loss peak to higher energy losses, there are also weak oscillations called extensive fine structures.

From the ionization absorption edge fine structure and extensive fine structure, information such as the valence bond state, coordination state, electronic structure, and charge distribution of the elements in the sample area can be obtained.

13.13 Electron energy loss spectrum

- Characteristics of electron energy loss spectrum and its applications

Using the electron energy filter imaging system, electron filter imaging with various energy losses can be selected, which can not only significantly improve the contrast between electron microscopy images and diffraction patterns, but also provide images of element distribution in the sample.

The figure below shows a comparison of the convergent beam electron diffraction pattern unfiltered and zero-loss filtered.

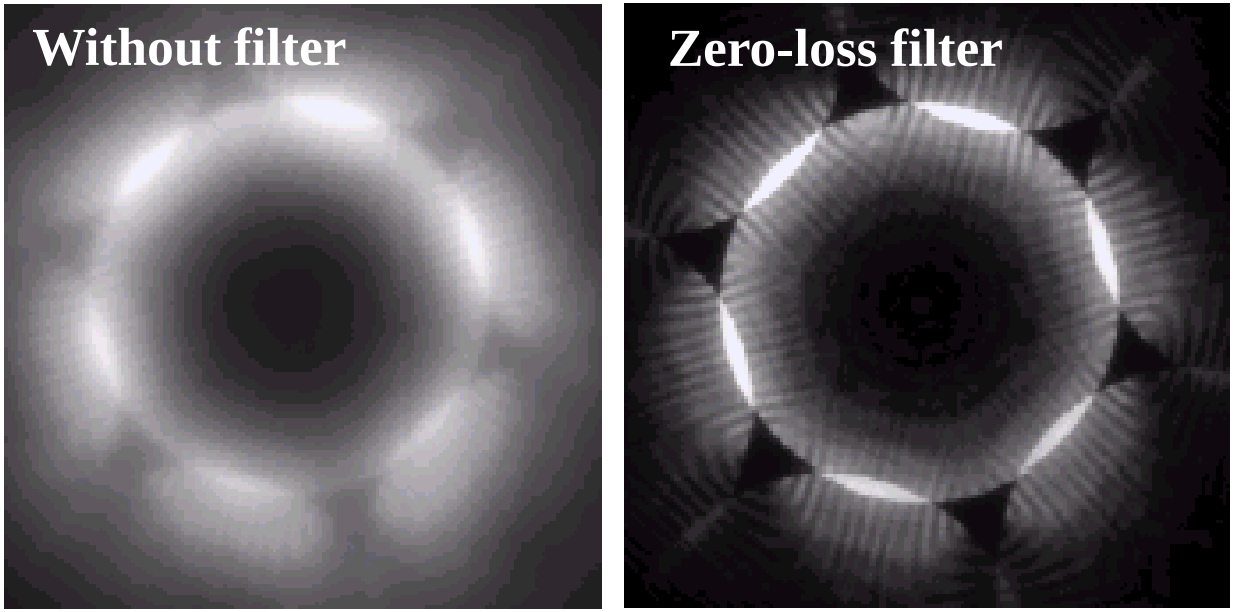

13.13 Electron energy loss spectrum

- Characteristics of electron energy loss spectrum and its applications

Electron energy loss spectroscopy can obtain spectra with a wide energy range, which can be used for both valence shell and inner shell research.

The energy resolution of the electron energy loss spectrum is very high, usually better than 1 eV, and the energy resolution is close to a constant, regardless of the excitation energy.

Generally speaking, the electron energy loss spectrum is not restricted by the electric dipole radiative transition selection rule, and the forbidden transition characteristics involved in non-electric dipole interactions can be studied under large momentum transfer conditions.

The electron energy loss spectrometer also has advantages in measuring differential scattering cross section and absolute optical oscillator intensity.

13.14 Scanning transmission electron microscope

- Overview

The relationship between material microstructure and defects and properties is an important part of research in the field of materials science. With the development of new materials towards nanoscale structures, research needs to be conducted at the nanometer or even atomic scale, which requires suitable analytical instruments and technical methods.

Scanning transmission electron microscopy (STEM) is a clever combination of TEM and SEM. A finely focused high-energy electron beam is used to scan the thin film sample and penetrate the sample. The detector receives various signals generated by the interaction between the electrons and the sample for imaging.

In the STEM operating mode, the high-angle annular dark field detector is used to receive elastically incoherent scattered electron imaging, and a dark field image with atomic-scale resolution, called a HAADF image, can be obtained. The contrast of this image depends only on the atomic number ***Z*** of the sample, so it is called a ***Z***-contrast image.

13.14 Scanning transmission electron microscope

- How scanning transmission electron microscopy works

The picture shows a STEM imaging. The finely focused high-energy electron beam is scanned point by point in the selected area of the sample through coil control. The annular detector below the sample receives Rusev scattered (elastic incoherent scattering) electrons into a dark field image.

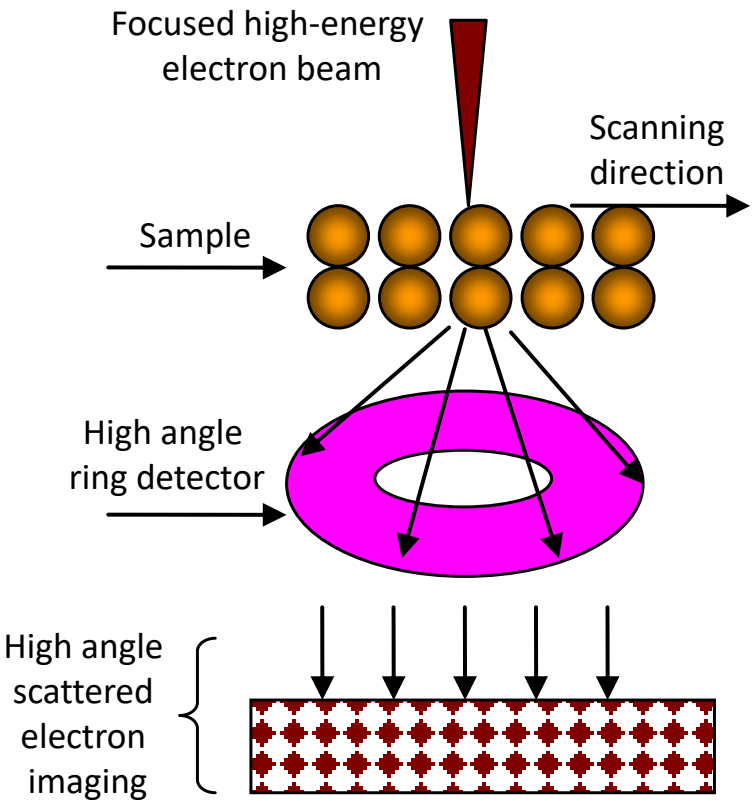

The brightness of a certain image point in the image depends on the number of elastically incoherent scattered electrons at its corresponding sample position. The number of elastically incoherently scattered electrons is proportional to the square of the sample atomic number (Z^2). Therefore, the high-angle annular dark field (HAADF) image is also called the atomic number contrast image (or ***Z***-contrast image)

13.14 Scanning transmission electron microscope

- Working characteristics of scanning transmission electron microscope

1) High resolution: Z-contrast images are imaged under incoherent conditions, and their image resolution is higher than those obtained under coherent conditions. Z contrast does not change with the thickness of the specimen or the defocus of the objective lens, and there will be no contrast inversion.

2) Sensitive to chemical composition: The brightness of the Z-contrast image point is proportional to the square (Z^2) of the sample atomic number at the corresponding point. The brightness and darkness in the Z-contrast image can reflect the size of the sample atomic number in the corresponding area. Z-contrast The image can directly display the distribution of phases with different chemical compositions, and can also intuitively reflect the arrangement of different atomic columns.

3) Simple interpretation of images: Z-contrast images are imaged under incoherent conditions and have a positive contrast transfer function. There is no contrast deviation or contrast inversion. The contrast of the image can directly reflect the objective object without the help of a computer. Simulate matching, which can directly determine the position of the atomic column.

13.14 Scanning transmission electron microscope

- Applications of scanning transmission electron microscopy

Z-contrast images have been used in material structure research in recent years due to their high resolution, sensitivity to chemical composition, and intuitive and easy-to-interpret images.

1) Atomic arrangement and defect structure at the film-base interface of thin film materials.

2) Arrangement of atomic columns in superlattice or superlattice structure.

3) Enrichment of certain elements at crystal defects (such as dislocations).

4) Research on nanometer core-shell structure.

5) Research on alloy precipitation process.

6) Structure and formation mechanism of quasicrystalline compounds